

Exotic double-charm molecular states with hidden or open strangeness and around 4.5 ~ 4.7 GeV

Fu-Lai Wang[†] and Xiang Liu^{✉*}

*School of Physical Science and Technology, Lanzhou University, Lanzhou 730000, China
and Research Center for Hadron and CSR Physics, Lanzhou University
and Institute of Modern Physics of CAS, Lanzhou 730000, China*



(Received 1 September 2020; accepted 16 October 2020; published 10 November 2020)

In this work, we investigate the interactions between the charmed-strange meson (D_s, D_s^*) in H -doublet and the (anti-)charmed-strange meson (D_{s1}, D_{s2}^*) in T -doublet, where the one boson exchange model is adopted by considering the S - D wave mixing and the coupled-channel effects. By extracting the effective potentials for the discussed $H_s\bar{T}_s$ and H_sT_s systems, we try to find the bound state solutions for the corresponding systems. We predict the possible hidden-charm hadronic molecular states with hidden strangeness, i.e., the $D_s^*\bar{D}_{s1} + c.c.$ states with $J^{PC} = 0^{--}, 0^{+-}$ and the $D_s^*\bar{D}_{s2} + c.c.$ states with $J^{PC} = 1^{--}, 1^{+-}$. Applying the same theoretical framework, we also discuss the H_sT_s systems. Unfortunately, the existence of the open-charm and open-strange molecular states corresponding to the H_sT_s systems can be excluded.

DOI: 10.1103/PhysRevD.102.094006

I. INTRODUCTION

Studying exotic hadronic states, which are very different from conventional mesons and baryons, is an intriguing research frontier full of opportunities and challenges in hadron physics. As an important part of hadron spectroscopy, exotic state can be as a good platform for deepening our understanding of nonperturbative behavior of quantum chromodynamics (QCD). Since the observation of the charmoniumlike state $X(3872)$ [1], a series of $X/Y/Z/P_c$ states have been observed in the past 17 years, which stimulated extensive discussions on exotic hadronic state assignments to them. Because of the masses of several $X/Y/Z/P_c$ states are close to the thresholds of two hadrons, it is natural to consider them as the candidates of the hadronic molecules, which is the reason why exploring hadronic molecular states has become popular. The theoretical and experimental progress on the hidden-charm multiquark states can be found by Refs. [2–8]. Among them, a big surprise is the observation from the LHCb Collaboration of three P_c states ($P_c(4312)$, $P_c(4440)$, and $P_c(4457)$) in 2019 [9], which provides

strong evidence to support these P_c states as the $\Sigma_c\bar{D}^{(*)}$ -type hidden-charm pentaquark molecules [10–16].

Before presenting our motivation, we first need to give a brief review of how these observed XYZ states were decoded as the corresponding hidden-charm molecular states. In 2003, $X(3872)$ was discovered by Belle [1]. For solving its low mass puzzle, the $D\bar{D}^*$ molecular state explanation was proposed in Ref. [17]. Later, more theoretical groups joined the discussion of whether $X(3872)$ can be assigned as $D\bar{D}^*$ molecular state [18,19], where more and more effects were added in realistic calculation of the $D\bar{D}^*$ interaction [20–25]. At the same time, another special XYZ state is $Z^+(4430)$, which was observed by Belle [26]. In Refs. [27–29], a dynamic calculation of $Z^+(4430)$ as $D^*\bar{D}_1^{(\prime)}$ molecular state was performed. Later, the observed $Y(4140)$ [30] also stimulated a universal molecular state explanation to $Y(3930)$ and $Y(4140)$ [31], which is due to the similarity between $Y(3930)$ [32] and $Y(4140)$ [30]. Additionally, $Y(4260)$ [33] as a $D\bar{D}_1$ molecular state was given [34] and discussed [35,36]. Besides $Y(4140)$ [30], the above studies on these typical charmoniumlike XYZ are mainly involved in hidden-charm hadronic molecular states without strangeness. These observed XYZ states also result in several systematic theoretical calculations of the interaction between charmed and anticharmed mesons [37–41]. Since the $Y(4274)$ [42] is observed in the $J/\psi\phi$ invariant mass spectrum and is just below the threshold of the $D_s\bar{D}_{s0}(2317)$ channel, the $Y(4274)$ fits well to be the S -wave $D_s\bar{D}_{s0}(2317)$ molecular state with $J^P = 0^-$ in Ref. [43]. Obviously, these studies

*Corresponding author.
xiangliu@lzu.edu.cn
[†]wangfl2016@lzu.edu.cn

Published by the American Physical Society under the terms of the Creative Commons Attribution 4.0 International license. Further distribution of this work must maintain attribution to the author(s) and the published article's title, journal citation, and DOI. Funded by SCOAP³.

enlarged our knowledge of hidden-charm hadronic molecular states with mass below 4.5 GeV.

In the past years, more XYZ states with higher mass were announced by many experiment collaborations [44–47]. In 2019, the BESIII Collaboration announced a white paper on the future physics program [48], where they plan to perform a detailed scan of cross sections between 4.0 and 4.6 GeV and take more data above 4.6 GeV. These new measurements will not only result in complement the higher radial and orbital charmonium family [49,50], but also provide us a good opportunity to study exotic state assignments to the XYZ states above 4.5 GeV.

For hidden-charm molecular states with and without strangeness, which has mass below 4.5 GeV, we have abundant theoretical study. However, our knowledge of hidden-charm molecular states above 4.5 GeV is still not enough. Considering this research status and future experimental plan, we propose to explore exotic double-charm molecular states with hidden or open strangeness existing in mass range around 4.5 ~ 4.7 GeV, which are relevant to the interactions between S -wave charmed-strange meson in H -doublet and P -wave (anti-)charmed-strange meson in T -doublet. Generally, the $H_s\bar{T}_s$ system corresponds to hidden-charm and hidden-strange hadronic molecular state with the $(c\bar{s})(\bar{c}s)$ configuration while the H_sT_s system is involved in open-charm and open-strange hadronic molecular state with the $(c\bar{s})(c\bar{s})$ configuration. In the following, the $H_s\bar{T}_s$ and H_sT_s systems will be main body of this work.

For obtaining the interaction information of the $H_s\bar{T}_s$ and H_sT_s systems, we apply one boson exchange (OBE) model [51,52] to deduce the effective potentials in coordinate space. With this effective potential reflecting the interaction of the $H_s\bar{T}_s$ and H_sT_s systems, we try to find bound state solutions of these discussed $H_s\bar{T}_s$ and H_sT_s systems, by which we may predict possible exotic double-charm molecular states with hidden or open strangeness around 4.5 ~ 4.7 GeV mass range. Further suggestion of experimental search for this new type of hadronic molecular states will be given.

This paper is organized as the follows. After introduction, we illustrate the deduction of the effective potentials of these discussed $H_s\bar{T}_s$ and H_sT_s systems in Sec. II. With this preparation, we present the numerical results of finding the bound state solutions in Sec. III. Finally, this work ends with a short summary in Sec. IV.

II. EFFECTIVE POTENTIALS INVOLVED IN THE $H_s\bar{T}_s$ AND H_sT_s SYSTEMS

In this section, we deduce the effective potentials in the coordinate space for the $H_s\bar{T}_s$ and H_sT_s systems,

where the OBE model is adopted in concrete calculation. Here, we need to emphasize that the OBE model was extensively applied to study these observed $X/Y/Z/P_c$ states [2,5].

A. Effective Lagrangians

When describing the interactions quantitatively at the hadronic level, we use the effective Lagrangian approach. For writing out the compact effective Lagrangians related to the charmed meson in H -doublet and the (anti-)charmed meson in T -doublet, it is convenient to introduce the superfields $H_a^{(Q)}$, $T_a^{(Q)\mu}$, $H_a^{(\bar{Q})}$, $T_a^{(\bar{Q})\mu}$, and their corresponding conjugate fields [34]. According to the heavy quark limit [53], the super-fields $H_a^{(Q)}$ and $T_a^{(Q)\mu}$ corresponding to the heavy-light meson $Q\bar{q}$ can be defined by [34]

$$H_a^{(Q)} = \mathcal{P}_+ (D_a^{*(Q)\mu} \gamma_\mu - D_a^{(Q)} \gamma_5),$$

$$T_a^{(Q)\mu} = \mathcal{P}_+ \left[D_{2a}^{*(Q)\mu\nu} \gamma_\nu - \sqrt{\frac{3}{2}} D_{1a\nu}^{(Q)} \gamma_5 \left(g^{\mu\nu} - \frac{1}{3} \gamma^\nu (\gamma^\mu - v^\mu) \right) \right],$$

respectively. Meanwhile, the antimeson $\bar{Q}q$ superfields $H_a^{(\bar{Q})}$ and $T_a^{(\bar{Q})\mu}$ can be obtained by the charge conjugate transformation for the superfields $H_a^{(Q)}$ and $T_a^{(Q)\mu}$ [34], where its expression denotes

$$H_a^{(\bar{Q})} = (\bar{D}_a^{*(\bar{Q})\mu} \gamma_\mu - \bar{D}_a^{(\bar{Q})} \gamma_5) \mathcal{P}_-,$$

$$T_a^{(\bar{Q})\mu} = \left[\bar{D}_{2a}^{*(\bar{Q})\mu\nu} \gamma_\nu - \sqrt{\frac{3}{2}} \bar{D}_{1a\nu}^{(\bar{Q})} \gamma_5 \left(g^{\mu\nu} - \frac{1}{3} (\gamma^\mu - v^\mu) \gamma^\nu \right) \right] \mathcal{P}_-.$$

Here, $\mathcal{P}_\pm = (1 \pm \not{v})/2$ denotes the projection operator, and $v^\mu = (1, 0, 0, 0)$ is the four velocity under the nonrelativistic approximation. Besides, their conjugate fields can be expressed as

$$\bar{X} = \gamma_0 X^\dagger \gamma_0, \quad X = H_a^{(Q)}, T_a^{(Q)\mu}, H_a^{(\bar{Q})}, T_a^{(\bar{Q})\mu}. \quad (2.1)$$

On the basis of the heavy quark symmetry, the chiral symmetry, and the hidden local symmetry [53–56], the compact effective Lagrangians depicting the interactions between the (anti-)charmed mesons and light pseudoscalar and vector mesons were constructed in Ref. [34], i.e.,

$$\begin{aligned}
\mathcal{L} = & ig\langle H_b^{(Q)} \mathbb{A}_{ba} \gamma_5 \bar{H}_a^{(Q)} \rangle + ig\langle \bar{H}_a^{(Q)} \mathbb{A}_{ab} \gamma_5 H_b^{(Q)} \rangle + ik\langle T_b^{(Q)\mu} \mathbb{A}_{ba} \gamma_5 \bar{T}_{a\mu}^{(Q)} \rangle + ik\langle \bar{T}_a^{(Q)\mu} \mathbb{A}_{ab} \gamma_5 T_{b\mu}^{(Q)} \rangle \\
& + [i\langle T_b^{(Q)\mu} \left(\frac{h_1}{\Lambda_\chi} D_\mu \mathbb{A} + \frac{h_2}{\Lambda_\chi} \mathcal{D} \mathbb{A}_\mu \right) \gamma_5 \bar{H}_a^{(Q)} \rangle + \text{H.c.}] + [i\langle \bar{H}_a^{(Q)} \left(\frac{h_1}{\Lambda_\chi} \mathbb{A} \bar{D}'_\mu + \frac{h_2}{\Lambda_\chi} \mathbb{A}_\mu \bar{D}' \right) \gamma_5 T_b^{(Q)\mu} \rangle + \text{H.c.}] \\
& + \langle iH_b^{(Q)} (\beta v^\mu (\mathcal{V}_\mu - \rho_\mu) + \lambda \sigma^{\mu\nu} F_{\mu\nu}(\rho))_{ba} \bar{H}_a^{(Q)} \rangle - \langle i\bar{H}_a^{(Q)} (\beta v^\mu (\mathcal{V}_\mu - \rho_\mu) - \lambda \sigma^{\mu\nu} F_{\mu\nu}(\rho))_{ab} H_b^{(Q)} \rangle \\
& + \langle iT_{b\lambda}^{(Q)} (\beta'' v^\mu (\mathcal{V}_\mu - \rho_\mu) + \lambda'' \sigma^{\mu\nu} F_{\mu\nu}(\rho))_{ba} \bar{T}_a^{(Q)\lambda} \rangle - \langle i\bar{T}_{a\lambda}^{(Q)} (\beta'' v^\mu (\mathcal{V}_\mu - \rho_\mu) - \lambda'' \sigma^{\mu\nu} F_{\mu\nu}(\rho))_{ab} T_b^{(Q)\lambda} \rangle \\
& + [\langle T_b^{(Q)\mu} (i\zeta_1 (\mathcal{V}_\mu - \rho_\mu) + \mu_1 \gamma^\nu F_{\mu\nu}(\rho))_{ba} \bar{H}_a^{(Q)} \rangle + \text{H.c.}] - [\langle \bar{H}_a^{(Q)} (i\zeta_1 (\mathcal{V}_\mu - \rho_\mu) - \mu_1 \gamma^\nu F_{\mu\nu}(\rho))_{ab} T_b^{(Q)\mu} \rangle + \text{H.c.}],
\end{aligned}$$

where the axial current \mathcal{A}_μ , the vector current \mathcal{V}_μ , and the vector meson field strength tensor $F_{\mu\nu}(\rho)$ are given by

$$\mathcal{A}_\mu = \frac{1}{2} (\xi^\dagger \partial_\mu \xi - \xi \partial_\mu \xi^\dagger)_\mu, \quad (2.2)$$

$$\mathcal{V}_\mu = \frac{1}{2} (\xi^\dagger \partial_\mu \xi + \xi \partial_\mu \xi^\dagger)_\mu, \quad (2.3)$$

$$F_{\mu\nu}(\rho) = \partial_\mu \rho_\nu - \partial_\nu \rho_\mu + [\rho_\mu, \rho_\nu], \quad (2.4)$$

respectively. Here, the pseudo-Goldstone and vector meson fields can be written as $\xi = \exp(i\mathbb{P}/f_\pi)$ and $\rho_\mu = ig_V \mathbb{V}_\mu / \sqrt{2}$, respectively. The light pseudoscalar meson matrix \mathbb{P} and the light vector meson matrix \mathbb{V}_μ have the standard form, i.e.,

$$\begin{aligned}
\mathbb{P} &= \begin{pmatrix} \frac{\pi^0}{\sqrt{2}} + \frac{\eta}{\sqrt{6}} & \pi^+ & K^+ \\ \pi^- & -\frac{\pi^0}{\sqrt{2}} + \frac{\eta}{\sqrt{6}} & K^0 \\ K^- & \bar{K}^0 & -\sqrt{\frac{2}{3}}\eta \end{pmatrix}, \\
\mathbb{V}_\mu &= \begin{pmatrix} \frac{\rho^0}{\sqrt{2}} + \frac{\omega}{\sqrt{2}} & \rho^+ & K^{*+} \\ \rho^- & -\frac{\rho^0}{\sqrt{2}} + \frac{\omega}{\sqrt{2}} & K^{*0} \\ K^{*-} & \bar{K}^{*0} & \phi \end{pmatrix}_\mu. \quad (2.5)
\end{aligned}$$

In addition, the covariant derivatives can be written as $D_\mu = \partial_\mu + \mathcal{V}_\mu$ and $D'_\mu = \partial_\mu - \mathcal{V}_\mu$.

With the above preparation, we can expand the compact effective Lagrangians to the leading order of the pseudo-Goldstone field. The expanded effective Lagrangians for the (anti-)charmed mesons and the exchanged light mesons are collected in Appendix A. Here, the normalized relations for the pseudoscalar charmed-strange meson D_s , the vector charmed-strange meson D_s^* , the axial-vector charmed-strange meson D_{s1} , and the tensor charmed-strange meson D_{s2}^* can be expressed as

$$\begin{aligned}
\langle 0 | D_s | c\bar{s}(0^-) \rangle &= \sqrt{m_{D_s}}, \\
\langle 0 | D_s^{*\mu} | c\bar{s}(1^-) \rangle &= \epsilon^\mu \sqrt{m_{D_s^*}}, \\
\langle 0 | D_{s1}^\mu | c\bar{s}(1^+) \rangle &= \epsilon^\mu \sqrt{m_{D_{s1}}}, \\
\langle 0 | D_{s2}^{*\mu\nu} | c\bar{s}(2^+) \rangle &= \zeta^{\mu\nu} \sqrt{m_{D_{s2}^*}},
\end{aligned}$$

respectively. Here, the polarization vector ϵ_m^μ ($m = 0, \pm 1$) with spin-1 field is written as $\epsilon_\pm^\mu = (0, \pm 1, i, 0)/\sqrt{2}$ and $\epsilon_0^\mu = (0, 0, 0, -1)$ in the static limit, and the polarization tensor $\zeta_m^{\mu\nu}$ ($m = 0, \pm 1, \pm 2$) with spin-2 field is constructed as $\zeta_m^{\mu\nu} = \sum_{m_1, m_2} \langle 1, m_1; 1, m_2 | 2, m \rangle \epsilon_{m_1}^\mu \epsilon_{m_2}^\nu$ [57].

B. Effective potentials

For getting the effective potentials in the coordinate space, we follow the standard strategy in Ref. [58]. First, we write out the scattering amplitudes $\mathcal{M}(h_1 h_2 \rightarrow h_3 h_4)$ of the involved scattering processes $h_1 h_2 \rightarrow h_3 h_4$. For the $\mathcal{D}'\bar{\mathcal{D}}$ systems, there exist the direct channel and crossed channel [27], which are depicted in Fig. 1, where the notations \mathcal{D}' and \mathcal{D} stand for two different charmed-strange mesons. In Fig. 1, according to requirement of the spin-parity conservation, we may determine the exchanged particles for certain hadron-hadron system in the framework of the OBE model. Here, we take the $D_s \bar{D}_{s1}$ system as an example to illustrate it. Since the $D_s D_s \eta$ and $D_s D_{s1} \eta$ vertexes are strictly forbidden by the spin-parity

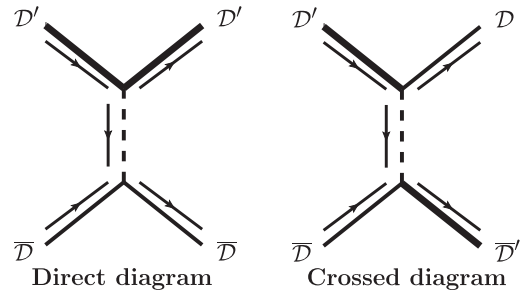


FIG. 1. The direct channel and crossed channel Feynman diagrams for the $\mathcal{D}'\bar{\mathcal{D}}$ systems. The thick (thin) lines stand for the charmed-strange mesons $\mathcal{D}'(\bar{\mathcal{D}})$, while the dashed lines represent the exchanged light mesons.

conservation, there only exists the ϕ exchange contribution to the direct and crossed channels for the $D_s\bar{D}_{s1}$ system.

Second, we have

$$\mathcal{V}_E^{h_1 h_2 \rightarrow h_3 h_4}(\mathbf{q}) = -\frac{\mathcal{M}(h_1 h_2 \rightarrow h_3 h_4)}{\sqrt{\prod_i 2m_i}} \quad (2.6)$$

with the Breit approximation [59,60] and the nonrelativistic normalization. Here, $\mathcal{V}_E^{h_1 h_2 \rightarrow h_3 h_4}(\mathbf{q})$ is the effective potentials in the momentum space, and $m_i (i = h_1, h_2, h_3, h_4)$ represent the masses of the initial and final states.

Thirdly, we need to get the effective potentials in the coordinate space $\mathcal{V}_E^{h_1 h_2 \rightarrow h_3 h_4}(\mathbf{r})$ by performing the Fourier transformation to $\mathcal{V}_E^{h_1 h_2 \rightarrow h_3 h_4}(\mathbf{q})$, i.e.,

$$\mathcal{V}_E^{h_1 h_2 \rightarrow h_3 h_4}(\mathbf{r}) = \int \frac{d^3 \mathbf{q}}{(2\pi)^3} e^{i\mathbf{q}\cdot\mathbf{r}} \mathcal{V}_E^{h_1 h_2 \rightarrow h_3 h_4}(\mathbf{q}) \mathcal{F}^2(q^2, m_E^2).$$

For compensating the off-shell effects of the exchanged light mesons and reflecting the inner structures of the interaction vertex, the form factor should be introduced in every interaction vertex [51,52]. We should indicate that the form factor also plays the role to regulate the effective potentials in the coordinate space since these effective potentials in the coordinate space have the singular delta-function terms [58]. In this work, we introduce the monopole type form factor $\mathcal{F}(q^2, m_E^2) = (\Lambda^2 - m_E^2) / (\Lambda^2 - q^2)$ in the OBE model [51,52]. Here, Λ , m_E , and q are the cutoff parameter, the mass, and the four momentum of the exchanged light mesons, respectively.

In order to obtain the effective potentials of these focused systems, we need to construct the flavor and spin-orbital wave functions of systems. For the hidden-charm and hidden-strange $\mathcal{D}'\bar{\mathcal{D}}$ molecular systems, we need distinguish the charge parity quantum numbers due to the charge conjugate transformation invariance. The flavor wave function $|I, I_3\rangle$ can be expressed as $|0, 0\rangle = |\mathcal{D}^+\mathcal{D}^- + c\mathcal{D}^+\mathcal{D}'^-\rangle / \sqrt{2}$ [20,22,38]. Here, we want to emphasize that there exists a relation of c and the C parity, i.e., $C = -c \cdot (-1)^{J_1 - J_2 - J}$, where the notations J , J_1 , and J_2 stand for the total angular momentum quantum numbers of the $\mathcal{D}'\bar{\mathcal{D}}$, the charmed-strange mesons \mathcal{D}' , and the charmed-strange mesons \mathcal{D} , respectively.

And then, we may get the spin-orbital wave functions $|^{2S+1}L_J\rangle$ for all of the investigated hidden-charm and hidden-strange molecular systems, i.e.,

$$|\mathcal{D}_0\bar{\mathcal{D}}_1\rangle = \sum_{m, m_L} C_{1m, Lm_L}^{J, M} \epsilon_m^\mu |Y_{L, m_L}\rangle, \quad (2.7)$$

$$|\mathcal{D}_0\bar{\mathcal{D}}_2\rangle = \sum_{m, m_L} C_{2m, Lm_L}^{J, M} \zeta_m^{\mu\nu} |Y_{L, m_L}\rangle, \quad (2.8)$$

$$|\mathcal{D}_1\bar{\mathcal{D}}_1\rangle = \sum_{m, m', m_S, m_L} C_{1m, 1m'}^{S, m_S} C_{Sm_S, Lm_L}^{J, M} \epsilon_m^\mu \epsilon_{m'}^\nu |Y_{L, m_L}\rangle, \quad (2.9)$$

$$|\mathcal{D}_1\bar{\mathcal{D}}_2\rangle = \sum_{m, m', m_S, m_L} C_{1m, 2m'}^{S, m_S} C_{Sm_S, Lm_L}^{J, M} \epsilon_m^\lambda \zeta_{m'}^{\mu\nu} |Y_{L, m_L}\rangle. \quad (2.10)$$

In the above expressions, the notations \mathcal{D}_0 , \mathcal{D}_1 , and \mathcal{D}_2 denote the charmed-strange mesons with the total angular momentum quantum numbers $J = 0, 1$, and 2 , respectively. The constant $C_{ab, cd}^{e, f}$ is the Clebsch-Gordan coefficient, and $|Y_{L, m_L}\rangle$ stands for the spherical harmonics function.

Through the above preparation, we can derive the effective potentials in the coordinate space for all of the investigated hidden-charm and hidden-strange systems, which are shown in Appendix B. We need to emphasize that the total effective potentials contain the direct channel and crossed channel contributions, which can be written in a general form, i.e.,

$$\mathcal{V}_{Total}(\mathbf{r}) = \mathcal{V}_D(\mathbf{r}) + c\mathcal{V}_C(\mathbf{r}), \quad (2.11)$$

where $\mathcal{V}_D(\mathbf{r})$ and $\mathcal{V}_C(\mathbf{r})$ are the effective potentials corresponding to the direct channel and crossed channel, respectively.

In the present work, we will also discuss the bound state properties of the S -wave $H_s T_s$ systems. Their OBE effective potentials can be related to the effective potentials of the $H_s \bar{T}_s$ systems by the G -parity rule [61], i.e.,

$$\mathcal{V}^{H_s T_s \rightarrow H_s T_s}(\mathbf{r}) = \sum_i G_i \mathcal{V}_i^{H_s \bar{T}_s \rightarrow H_s \bar{T}_s}(\mathbf{r}), \quad (2.12)$$

where G_i is the G -parity of some exchanged mesons. We need to emphasize that we only need to consider the direct diagram contribution to the $H_s T_s$ systems since the charge conjugate transformation invariance for the $H_s T_s$ systems does not exist.

III. NUMERICAL RESULTS

For describing the interactions quantitatively, we need the values of the coupling constants. The pionic coupling constant g can be determined by reproducing the experimental width of the process $D^{*+} \rightarrow D^0 \pi^+$ [62,63]. With the available experimental information, the authors extracted the coupling constant $h' = (h_1 + h_2) / \Lambda_\chi$ [55]. According to the vector meson dominance mechanism [63], the coupling constants β , ζ_1 , μ_1 , and g_V can be obtained [63,64]. Among them, the coupling constants ζ_1 and μ_1 are consistent with the numerical results in Refs. [65,66]. The coupling constant λ may be fixed by comparing the form factor obtained from the lattice QCD with this calculated via the light cone sum rule [63]. In addition, the coupling constants with the charmed meson in T -doublet can be estimated with the quark model in Refs. [58,67,68].

TABLE I. The summary of the coupling constants and the hadron masses adopted in our calculations. Unit of the coupling constants h' , λ , λ'' , and μ_1 is GeV^{-1} , and the coupling constant f_π is given in units of GeV .

	(g, k)	$ h' $	f_π	(β, β'')
Coupling constants	(0.59, 0.59)	0.55	0.132	(-0.90, 0.90)
	(λ, λ'')	$ \zeta_1 $	μ_1	g_V
	(-0.56, 0.56)	0.20	0	5.83
	η	ϕ	D_s	D_s^*
Hadron masses (MeV)	547.86	1019.46	1968.34	2112.20
	D_{s1}	D_{s2}^*		
	2535.11	2569.10		

Meanwhile, the corresponding phase factors between these coupling constants related to the effective potentials in the direct channels are fixed with the quark model [69]. In addition, we also need the parameters of the hadron masses [70]. The values of the coupling constants and the hadron masses are listed in Table I. Thus, the cutoff Λ in the form factor is only one free parameter in our numerical analysis, we attempt to find the loosely bound solutions by varying the cutoff parameters Λ from 1 to 5 GeV in the following.¹ In this work, we take cutoff range around 1 GeV to discuss possible hadron molecular states with hidden-charm and hidden-strange.

A. The hidden-charm and hidden-strange molecular systems

The hadronic molecular state is a loosely bound state, where the binding energy should be tens of MeV, and the typical size should be larger than the size of all the included hadrons [71]. The above criteria may provide us the critical information to identify the hadronic molecular candidates. Besides, it is important to note that the S -wave bound states should first appear since there exist the repulsive centrifugal potential $\ell(\ell+1)/2\mu r^2$ for the higher partial wave states (μ and ℓ respectively are the reduced mass and the angular momentum quantum number for the investigated system). Thus, we are mainly interested in the S -wave $H_s \bar{T}_s$ systems in this work.

In fact, the S - D wave mixing effect may play an important role to modify the bound properties of the deuteron, which

¹For the $Y(4274)$ [42], the spin-parity quantum number $J^{PC} = 1^{++}$ was measured by the LHCb Collaboration later [44], which is not consistent with the J^{PC} quantum number corresponding to the assignment of the S -wave $D_s \bar{D}_{s0}$ (2317) molecular state even. Considering this situation, we did not adopt the observed $Y(4274)$ to fix the Lambda cutoff in this work. As is well known, the deuteron is a loosely bound state composed of a proton and a neutron, and may be regarded as an ideal molecular state. By reproducing the binding energy and root-mean-square radius of deuteron with the OBE potential model, the Λ cutoff should be around 1 GeV [51,52,58].

TABLE II. The relevant quantum numbers J^P and possible channels $|^{2S+1}L_J\rangle$ involved in the S -wave $H_s \bar{T}_s$ systems. Here, “...” means that the S -wave components for the corresponding channels do not exist.

J^P	$D_s \bar{D}_{s1}$	$D_s \bar{D}_{s2}^*$	$D_s^* \bar{D}_{s1}$	$D_s^* \bar{D}_{s2}^*$
0^-	$ ^1S_0\rangle/ ^5D_0\rangle$...
1^-	$ ^3S_1\rangle/ ^3D_1\rangle$...	$ ^3S_1\rangle/ ^3,5D_1\rangle$	$ ^3S_1\rangle/ ^3,5,7D_1\rangle$
2^-	...	$ ^5S_2\rangle/ ^5D_2\rangle$	$ ^5S_2\rangle/ ^1,3,5D_2\rangle$	$ ^5S_2\rangle/ ^3,5,7D_2\rangle$
3^-	$ ^7S_3\rangle/ ^3,5,7D_3\rangle$

may be regarded as an ideal molecular state [51,52,58]. In this work, we also consider the S - D wave mixing effect to the S -wave $H_s \bar{T}_s$ systems. The relevant spin-orbit wave functions $|^{2S+1}L_J\rangle$ are summarized in Table II, where S , L , and J denote the spin, angular momentum, and total angular momentum quantum numbers, respectively.

By solving the Schrödinger equation

$$-\frac{1}{2\mu} \left(\nabla^2 - \frac{\ell(\ell+1)}{r^2} \right) \psi(r) + V(r)\psi(r) = E\psi(r), \quad (3.1)$$

we can find bound state solutions of these discussed systems. Here, $\nabla^2 = \frac{1}{r^2} \frac{\partial}{\partial r} r^2 \frac{\partial}{\partial r}$ and $\mu = \frac{m_1 m_2}{m_1 + m_2}$ as the reduced mass for the investigated system. The bound state solutions include the binding energy E and the radial wave function $\psi(r)$. In addition, we can further calculate the root-mean-square radius r_{RMS} and the probability of the individual channel P_i . In the following, we present the numerical results for single channel and coupled-channel cases, respectively.

1. The single channel analysis

In our numerical analysis, we first give the results without considering the S - D wave mixing effect. After that, we further take into account the S - D wave mixing effect, and repeat the numerical analysis. For the S -wave

TABLE III. Bound state solutions for the S -wave $D_s \bar{D}_{s1}$ system. The cutoff Λ , the binding energy E , and the root-mean-square radius r_{RMS} are in units of GeV, MeV, and fm, respectively. Here, we label the major probability for the corresponding channels in a bold manner, and the second column shows the numerical results without considering the S - D wave mixing effect while the last column shows the relevant results with the S - D wave mixing effect.

J^{PC}	Λ	E	r_{RMS}	Λ	E	r_{RMS}	$P(^3S_1/^3D_1)$
1^{--}	4.56	-0.30	4.73	4.56	-0.30	4.73	100.00 / $o(0)$
	4.78	-0.67	3.63	4.78	-0.67	3.63	100.00 / $o(0)$
	5.00	-1.15	2.89	5.00	-1.15	2.89	100.00 / $o(0)$
1^{+-}	3.85	-0.31	4.72	3.85	-0.31	4.72	100.00 / $o(0)$
	4.43	-2.26	2.12	4.43	-2.26	2.12	100.00 / $o(0)$
	5.00	-5.07	1.46	5.00	-5.07	1.46	100.00 / $o(0)$

TABLE IV. Bound state solutions for the S -wave $D_s\bar{D}_{s2}^*$ system. Conventions are the same as Table III. Here, “ \times ” indicates no binding energy when scanning the Λ range 1–5 GeV.

J^{PC}	Λ	E	r_{RMS}	Λ	E	r_{RMS}	$P(^5S_2/^5D_2)$
2^{--}	\times	\times	\times	4.70	-0.22	5.00	99.87 /0.13
	\times	\times	\times	4.76	-2.87	1.81	99.53 /0.47
	\times	\times	\times	4.82	-9.76	1.00	99.07 /0.93
2^{-+}	2.44	-0.31	4.69	2.41	-0.34	4.58	99.99 /0.01
	2.52	-2.95	1.87	2.49	-3.35	1.76	99.97 /0.03
	2.60	-10.16	1.06	2.56	-10.26	1.05	99.93 /0.07

$H_s\bar{T}_s$ systems, the relevant numerical results are collected in Tables III–VI within the OBE model, which include the cutoff parameter Λ , the binding energy E , the root-mean-square radius r_{RMS} , and the probability of the individual channel P_i .

Since the $D_s D_s \eta$ and $D_s D_{s1} \eta$ vertexes are forbidden by the spin-parity conservation, there only exist the ϕ exchange contribution to the direct and crossed channels for the $D_s \bar{D}_{s1}$ system. By performing numerical calculations, we can find that there exist the loosely bound state solutions for the S -wave $D_s \bar{D}_{s1}$ states with $J^{PC} = 1^{--}$ and 1^{-+} when the cutoff parameters Λ are larger than 4.56 GeV and 3.85 GeV, respectively. However, such cutoff parameters are unusual and deviate from the reasonable range around 1.00 GeV [51,52,58], which reflects that the ϕ exchange interaction is not strong enough to generate the

bound states for the S -wave $D_s \bar{D}_{s1}$ states with $J^{PC} = 1^{--}$ and 1^{-+} . Thus, these states as the candidates of the hadronic molecular states are no priority. Besides, we also notice that the $D_s \bar{D}_{s1}$ system without and with the S - D wave mixing effect have the same bound state properties in our calculation, which is not surprising since the contribution of the tensor forces from the S - D wave mixing effect for the $D_s \bar{D}_{s1}$ interactions disappears.

For the S -wave $D_s \bar{D}_{s2}^*$ state with $J^{PC} = 2^{--}$, there do not exist the loosely bound state solutions if we only consider the S -wave component until we increase the cutoff parameter Λ to be around 5 GeV. There exist weakly bound state solutions when the value of the cutoff parameter is taken around 4.70 GeV if adding the contributions of the S - D wave mixing effect. For the S -wave $D_s \bar{D}_{s2}^*$ state with $J^{PC} = 2^{-+}$, we can find the loosely bound state solutions when the cutoff parameter Λ larger than 2.40 GeV, even if the S - D wave mixing effect is included in our calculation. According to our quantitative analysis, it is obvious that the corresponding cutoff parameters are far away from the usual value around 1 GeV for the S -wave $D_s \bar{D}_{s2}^*$ bound states with $J^{PC} = 2^{--}$ and 2^{-+} [51,52,58]. Here, the large cutoff parameter means that the attractive forces are not strong enough to form these loosely bound states. Thus, we conclude that our numerical results disfavor the existence of the hadronic molecular state candidates for the S -wave $D_s \bar{D}_{s2}^*$ states with $J^{PC} = 2^{--}$ and 2^{-+} .

TABLE V. Bound state solutions for the S -wave $D_s^* \bar{D}_{s1}$ system. Conventions are the same as Table III.

J^{PC}	Λ	E	r_{RMS}	Λ	E	r_{RMS}	$P(^1S_0/^5D_0)$
0^{--}	1.68	-0.41	4.14	1.68	-0.42	4.09	100.00 / $o(0)$
	1.72	-4.59	1.38	1.72	-4.63	1.38	100.00 / $o(0)$
	1.75	-10.27	0.95	1.75	-10.32	0.95	100.00 / $o(0)$
0^{-+}	1.55	-0.22	4.98	1.55	-0.35	4.48	99.95 /0.05
	1.59	-3.91	1.57	1.59	-4.28	1.51	99.89 /0.11
	1.62	-9.75	1.03	1.62	-10.26	1.01	99.87 /0.13
J^{PC}	Λ	E	r_{RMS}	Λ	E	r_{RMS}	$P(^3S_1/^3D_1/^5D_1)$
1^{-+}	1.83	-0.30	4.63	1.82	-0.23	4.95	99.96 /0.04/ $o(0)$
	1.89	-3.84	1.59	1.88	-3.54	1.66	99.89 /0.11/ $o(0)$
	1.94	-10.06	1.03	1.93	-9.53	1.05	99.86 /0.13/ $o(0)$
1^{--}	2.00	-0.32	4.51	1.99	-0.23	4.90	100.00 / $o(0)$ / $o(0)$
	2.07	-4.20	1.47	2.06	-4.01	1.51	99.99 / $o(0)$ / $o(0)$
	2.13	-10.82	0.95	2.12	-10.71	0.95	99.97 /0.01/ $o(0)$
J^{PC}	Λ	E	r_{RMS}	Λ	E	r_{RMS}	$P(^5S_2/^1D_2/^3D_2/^5D_2)$
2^{--}	3.313	-0.33	4.46	3.119	-0.29	4.67	99.55 /0.40/ $o(0)$ / $o(0)$
	3.316	-5.60	1.23	3.125	-3.81	1.55	98.28 /1.59/ $o(0)$ / $o(0)$
	3.318	-13.00	0.78	3.130	-10.75	0.92	97.03 /2.81/ $o(0)$ / $o(0)$
2^{-+}	2.96	-0.29	4.84	2.86	-0.31	4.76	99.97 /0.02/ $o(0)$ / $o(0)$
	3.20	-3.27	1.87	3.04	-3.07	1.92	99.85 /0.09/ $o(0)$ / $o(0)$
	3.43	-10.00	1.17	3.22	-10.20	1.15	99.59 /0.21/ $o(0)$ / $o(0)$

TABLE VI. Bound state solutions for the S -wave $D_s^* \bar{D}_{s2}^*$ system. Conventions are the same as Table III.

J^{PC}	Λ	E	r_{RMS}	Λ	E	r_{RMS}	$P(^3S_1/^3D_1/^5D_1/^7D_1)$
1^{--}	1.70	-0.60	3.65	1.69	-0.50	3.90	99.97 /0.02/ $o(0)$ /0.01
	1.74	-4.15	1.49	1.73	-4.01	1.51	99.94 /0.05/ $o(0)$ /0.01
	1.78	-10.68	0.96	1.77	-10.69	0.96	99.91 /0.08/ $o(0)$ /0.01
1^{-+}	1.61	-0.56	3.76	1.60	-0.28	4.67	99.99 / $o(0)$ / $o(0)$ /0.01
	1.65	-5.12	1.36	1.64	-4.28	1.48	99.96 /0.01/ $o(0)$ /0.03
	1.68	-11.56	0.93	1.67	-10.37	0.98	99.94 /0.02/ $o(0)$ /0.04
J^{PC}	Λ	E	r_{RMS}	Λ	E	r_{RMS}	$P(^5S_2/^3D_2/^5D_2/^7D_2)$
2^{-+}	2.67	-0.28	4.69	2.63	-0.26	4.77	99.99 / $o(0)$ /0.01/ $o(0)$
	2.86	-3.58	1.60	2.80	-3.68	1.58	99.96 / $o(0)$ /0.04/ $o(0)$
	3.05	-10.08	0.98	2.96	-10.43	0.96	99.91 / $o(0)$ /0.09/ $o(0)$
2^{--}	1.91	-0.47	4.06	1.90	-0.26	4.82	99.99 / $o(0)$ /0.01/ $o(0)$
	1.96	-3.57	1.65	1.96	-3.81	1.60	99.97 / $o(0)$ /0.03/ $o(0)$
	2.01	-10.20	1.01	2.01	-10.62	1.00	99.96 / $o(0)$ /0.04/ $o(0)$
J^{PC}	Λ	E	r_{RMS}	Λ	E	r_{RMS}	$P(^7S_3/^3D_3/^5D_3/^7D_3)$
3^{--}	4.18	-0.28	4.87	3.87	-0.29	4.80	99.96 /0.03/ $o(0)$ /0.01
	4.59	-2.56	2.07	4.04	-1.97	2.32	99.83 /0.13/ $o(0)$ /0.04
	5.00	-6.36	1.40	4.20	-9.89	1.15	98.87 /0.97/ $o(0)$ /0.16

In this work, we need to focus on the q^4 correction terms in the effective potentials, the expressions of these correction terms are a little tricky (see Eq. (B5) of the Appendix B for more details). Through our numerical analysis for the $D_s \bar{D}_{s2}^*$ system, we can obtain an inequality $\Lambda(J^{PC} = 2^{--}) > \Lambda(J^{PC} = 2^{-+})$ when taking the same binding energy. This difference is caused by the q^4 correction terms in the effective potentials. Usually, a loosely bound state with smaller cutoff parameter corresponds to the more attractive interaction, which means that the q^4 correction terms in the effective potentials are favorable for forming the $D_s \bar{D}_{s2}^*$ molecular state with $J^{PC} = 2^{-+}$. In contrast, these correction terms are unfavorable for forming the $D_s \bar{D}_{s2}^*$ state with $J^{PC} = 2^{--}$. Based on the analysis mentioned above, it is clear that the q^4 correction terms in the interactions play an important role to modify the behavior of the loosely bound state in some cases.

Besides the S -wave $D_s \bar{D}_{s1}(\bar{D}_{s2}^*)$ systems, we also investigate the bound state properties of the S -wave $D_s^* \bar{D}_{s1}(\bar{D}_{s2}^*)$ systems in the current work. For the $D_s^* \bar{D}_{s1}(\bar{D}_{s2}^*)$ systems, we notice that the η and ϕ exchange contributions to the direct and crossed diagrams are also allowed, and their interactions are simultaneously associated with the total angular momentum J and the charge parity C .

From the numerical results for the S -wave $D_s^* \bar{D}_{s1}$ and $D_s^* \bar{D}_{s2}^*$ systems with and without considering the S - D wave mixing effect, we can find several interesting results:

- (1) When tuning the cutoff parameters Λ from 1 GeV to 5 GeV, we can obtain the loosely bound solutions for the $D_s^* \bar{D}_{s1}$ states with $J^{PC} = 0^{--}, 0^{-+}, 1^{--}, 1^{-+}, 2^{--}, 2^{-+}$ and the $D_s^* \bar{D}_{s2}^*$ states with $J^{PC} = 1^{--}, 1^{-+}, 2^{--}, 2^{-+}, 3^{--}$, where the S -wave $D_s^* \bar{D}_{s1}$ and $D_s^* \bar{D}_{s2}^*$ states with lower spin can be bound more tightly;
- (2) If strictly considering this criterion of the cutoff value Λ around 1 GeV [51,52,58], our results disfavor the existence of the hidden-charm and hidden-strange tetraquark molecular candidates for the S -wave $D_s^* \bar{D}_{s1}(\bar{D}_{s2}^*)$ states;
- (3) If the cutoff Λ smaller than 1.70 GeV is a reasonable input parameter,² our results suggest that the $D_s^* \bar{D}_{s1}$ states with $J^{PC} = 0^{--}, 0^{-+}$ and the $D_s^* \bar{D}_{s2}^*$ states with $J^{PC} = 1^{--}, 1^{-+}$ are good candidates of the hidden-charm and hidden-strange molecular states. Here, we need to emphasize that the $D_s^* \bar{D}_{s1}$ state with $J^{PC} = 0^{--}$ and the $D_s^* \bar{D}_{s2}^*$ state with $J^{PC} = 1^{-+}$ are very different from the $D_s^* \bar{D}_{s1}$ state with $J^{PC} = 0^{-+}$ and the $D_s^* \bar{D}_{s2}^*$ state with $J^{PC} = 1^{--}$, since they have the exotic spin-parity quantum

²In this work, we take a Λ range from 1 GeV to 5 GeV when finding the bound state solution of these discussed systems. According to the experience of studying deuteron, the cutoff value should not be far away from 1 GeV. Thus, in this work, we take such so-called criteria to make discussion of possible molecular states.

numbers apparently different from the conventional hadrons.

- (4) The S - D wave mixing effect plays a minor role in generating the S -wave $D_s^* \bar{D}_{s1}$ and $D_s^* \bar{D}_{s2}^*$ bound states in many cases.

2. The coupled-channel analysis

In this subsection, we discuss the $H_s \bar{T}_s$ systems with $J = 1, 2$ by considering the coupled-channel effect. In the coupled-channel approach, we need to emphasize that the binding energy E is determined by the lowest mass threshold among various involved channels [71]. The relevant numerical results for the $H_s \bar{T}_s$ coupled systems with $J^{PC} = 1^{--}, 1^{+-}, 2^{--}, 2^{+-}$ for the different lowest mass thresholds are given in Table VII.

By comparing the numerical results of the single channel and coupled-channel cases, it is obvious that the bound state properties will change accordingly after considering the coupled-channel effect, i.e., the cutoff parameters in the coupled-channel analysis are smaller than that in the single channel analysis with the same binding energy in many cases, especially for the $D_s \bar{D}_{s1}$ state with $J^{PC} = 1^{--}$. However, our result indicates that the coupled-channel effect to the S -wave $H_s \bar{T}_s$ systems is not obvious.

We may predict the existence of four possible hidden-charm and hidden-strange molecular states, which are the $D_s^* \bar{D}_{s1}$ states with $J^{PC} = 0^{--}, 0^{-+}$ and the $D_s^* \bar{D}_{s2}^*$ states with $J^{PC} = 1^{--}, 1^{-+}$. These predictions can be accessible at future experiment. Moreover, the $D_s^* \bar{D}_{s1}$ state with $J^{PC} = 0^{--}$ and the $D_s^* \bar{D}_{s2}^*$ state with $J^{PC} = 1^{-+}$ have the typical exotic spin-parity quantum numbers, which can be distinguished with conventional mesons.

B. The open-charm and open-strange molecular systems

In the above subsection, we mainly discussed the bound state properties of the S -wave $H_s \bar{T}_s$ systems, which stimulates our interest to investigate the behavior of the open-charm and open-strange molecular systems composed by a charmed-strange meson in H -doublet and a charmed-strange meson in T -doublet, which have typical exotic state configurations totally different from the conventional hadrons.

1. The single channel analysis

In the following, we try to search for the bound state solutions for the S -wave $H_s \bar{T}_s$ systems by solving the coupled-channel Schrödinger equation. When considering

TABLE VII. Bound state solutions for the S -wave $H_s \bar{T}_s$ coupled systems. Conventions are the same as Table III. Here, “Threshold” represents the lowest mass threshold, and “...” means that the S -wave components for the corresponding channels do not exist or the corresponding channels below the threshold considered.

J^{PC}	Threshold	Λ	E	r_{RMS}	$P(D_s \bar{D}_{s1} / D_s \bar{D}_{s2}^* / D_s^* \bar{D}_{s1} / D_s^* \bar{D}_{s2}^*)$
1 ⁻⁻	$D_s \bar{D}_{s1}$	1.92	-0.32	4.42	91.19 /.../o(0)/8.18
		1.93	-3.38	1.47	72.37 /.../o(0)/27.63
		1.94	-9.24	0.83	57.50 /.../o(0)/ 42.50
	$D_s^* \bar{D}_{s1}$	1.86	-2.17	0.56	.../.../o(0)/ 100.00
		1.87	-6.01	0.54	.../.../o(0)/ 100.00
		1.88	-10.06	0.52	.../.../o(0)/ 100.00
1 ⁺⁻	$D_s \bar{D}_{s1}$	1.87	-0.50	3.36	69.27 /.../o(0)/30.73
		1.88	-8.88	0.61	25.86/.../o(0)/ 74.14
		1.89	-20.56	0.39	16.13/.../o(0)/ 83.87
	$D_s^* \bar{D}_{s1}$	1.74	-0.43	0.58	.../.../o(0)/ 100.00
		1.75	-5.27	0.55	.../.../o(0)/ 100.00
		1.76	-10.46	0.52	.../.../o(0)/ 100.00
2 ⁻⁻	$D_s \bar{D}_{s2}^*$	2.27	-3.24	0.28	.../o(0)/o(0)/ 100.00
		2.28	-13.95	0.27	.../o(0)/o(0)/ 100.00
		2.29	-25.24	0.26	.../o(0)/o(0)/ 100.00
	$D_s^* \bar{D}_{s1}$	2.11	-3.89	0.54	.../.../o(0)/ 100.00
		2.12	-8.00	0.51	.../.../o(0)/ 100.00
		2.13	-12.41	0.49	.../.../o(0)/ 100.00
2 ⁺⁻	$D_s \bar{D}_{s2}^*$	2.40	-0.33	4.61	.../ 99.94 /0.06/o(0)
		2.49	-3.47	1.72	.../ 99.81 /0.19/o(0)
		2.57	-10.76	1.01	.../ 99.64 /0.36/o(0)
	$D_s^* \bar{D}_{s1}$	2.86	-0.31	4.74	.../.../ 100.00 /o(0)
		3.04	-3.07	1.90	.../.../ 100.00 /o(0)
		3.22	-10.18	1.13	.../.../ 100.00 /o(0)

TABLE VIII. Bound state solutions for the S -wave $H_s T_s$ systems. Conventions are the same as Table III.

$D_s^* D_{s1}(J^P = 2^-)$						
Λ	E	r_{RMS}	Λ	E	r_{RMS}	$P(^5S_2/^1D_2/^3D_2/^5D_2)$
4.69	-1.73	1.90	3.32	-0.64	3.49	97.11 /0.13/ $o(0)$ /2.76
4.70	-5.74	0.98	3.36	-4.90	1.33	93.64 /0.27/ $o(0)$ /6.09
4.71	-10.84	0.70	3.39	-10.27	0.93	91.95 /0.33/ $o(0)$ /7.72
$D_s^* D_{s2}^*(J^P = 2^-)$						
Λ	E	r_{RMS}	Λ	E	r_{RMS}	$P(^5S_2/^3D_2/^5D_2/^7D_2)$
\times	\times	\times	4.66	-0.25	4.85	98.21 /0.49/0.98/0.33
\times	\times	\times	4.76	-3.52	1.62	94.49 /1.44/3.06/1.02
\times	\times	\times	4.86	-10.32	0.99	91.66 /2.09/4.69/1.56
$D_s^* D_{s2}^*(J^P = 3^-)$						
Λ	E	r_{RMS}	Λ	E	r_{RMS}	$P(^7S_3/^3D_3/^5D_3/^7D_3)$
4.20	-2.59	1.53	3.14	-0.65	3.46	96.94 /0.09/0.31/3.86
4.21	-6.99	0.90	3.17	-3.89	1.48	93.83 /0.13/0.44/5.60
4.22	-12.40	0.66	3.20	-9.38	0.97	91.80 /0.16/0.58/7.47

the S - D wave mixing effect and scanning the cutoff parameters Λ from 1 GeV to 5 GeV, we list these typical values of the cutoff parameter Λ , the binding energy E , the root-mean-square radius r_{RMS} , and the probability of the individual channel P_i for the S -wave $H_s T_s$ systems in Table VIII. According to the theoretical results of studying the deuteron via the OBE model, the cutoff parameter Λ should be around 1 GeV [51,52,58]. If taking this criterion, our results disfavor the existence of the open-charm and open-strange molecular states for the S -wave $D_s^{(*)} D_{s1}(D_{s2}^*)$ systems since the cutoff parameter Λ is obviously far away from 1 GeV.

2. The coupled-channel analysis

Similar to the S -wave $H_s \bar{T}_s$ systems, we also present the bound state properties for the S -wave $H_s T_s$ coupled-channel systems in Table IX. Nevertheless, it is clear that the coupled-channel effect plays a positive but minor effect to generate these S -wave $D_s^{(*)} D_{s1}(D_{s2}^*)$ bound states, where

the corresponding cutoff is deviated from the usual value around 1 GeV for these investigated open-charm and open-strange systems [51,52,58]. It means that S -wave bound states for the $H_s T_s$ systems do not exist even the coupled-channel effect is included.

In short summary, since the attractive interactions between a charmed-strange meson in H -doublet and a charmed-strange meson in T -doublet are not strong enough to make the hadronic component bound together when taking reasonable input parameters. Thus, we conclude that the quantitative analysis does not support the existence of the open-charm and open-strange tetraquark molecular candidates with the S -wave $D_s^{(*)} D_{s1}(D_{s2}^*)$ systems, such qualitative conclusion can be further tested in future experiments and other theoretical approaches.

IV. SUMMARY

Exploring the exotic hadronic states has become an intriguing research issue full of challenges and opportunities, which has been inspired by the abundant observations of a series of $X/Y/Z/P_c$ states since 2003 [2,5]. Among different exotic hadronic configurations, hadronic molecular state has aroused heated discussion. By the efforts from both theorist and experimentalist, the properties of hidden-charm molecular states with masses below 4.5 GeV, which are from the interaction between charmed meson and anti-charmed meson, become more and more clearer.

Recently, the observation of XYZ charmoniumlike states in experiment collaborations [44–47] and the announced white paper on the future physics program by the BESIII Collaboration [48] show that hunting new XYZ charmoniumlike states with mass above 4.5 GeV becomes possible. Considering the close relation of XYZ states with hidden-charm hadronic molecular states, we propose to perform theoretical study of hidden-charm hadronic molecular states composed of the charmed-strange meson in H -doublet and the anticharmed-strange meson in T -doublet. The discussed hidden-charm and hidden-strange hadronic molecular states just exist in the mass range around 4.5 ~ 4.7 GeV. We predict the existence of the $D_s^* \bar{D}_{s1}$ molecular states with $J^{PC} = 0^{--}, 0^{-+}$ and the $D_s^* \bar{D}_{s2}^*$ molecular states with $J^{PC} = 1^{--}, 1^{-+}$. Here, the

TABLE IX. Bound state solutions for the S -wave $H_s T_s$ coupled-channel systems. Conventions are the same as Table VII.

J^P	Threshold	Λ	E	r_{RMS}	$P(D_s D_{s1}/D_s D_{s2}^*/D_s^* D_{s1}/D_s^* D_{s2}^*)$
2^-	$D_s D_{s2}^*$	2.92	-1.75	1.62	\dots / 60.58 / 34.02 / 5.40
		2.93	-7.86	0.67	\dots / 47.20 / 45.48 / 7.32
		2.94	-15.15	0.47	\dots / 42.22 / 49.65 / 8.13
	$D_s^* D_{s1}$	3.25	-0.30	4.51	\dots / \dots / 99.88 / 0.12
		3.29	-4.45	1.36	\dots / \dots / 99.58 / 0.42
		3.32	-10.19	0.91	\dots / \dots / 99.37 / 0.63

$D_s^* \bar{D}_{s1}$ molecular state with $J^{PC} = 0^{--}$ and the $D_s^* \bar{D}_{s2}^*$ molecular state with $J^{PC} = 1^{-+}$ have the exotic spin-parity quantum numbers, which can be totally distinguished with the conventional meson states.

We also extend our theoretical framework to study open-charm and open-strange molecular systems, which have components, a charmed-strange meson in H -doublet and a charmed-strange meson in T -doublet. However, our calculation does not support the existence of such hadronic molecular states.

The possible hidden-charm hadronic molecular states with hidden strangeness can be searched in their possible two-body strong decay channels, where they can decay into a charmonium plus a ϕ meson, and a charmed-strange meson plus an anticharmed-strange meson if kinetically allowed, i.e., $\eta_c(1S)\phi$, $J/\psi\phi$, $\chi_{cJ}(1P)\phi$ ($J = 0, 1, 2$), $D_s \bar{D}_s$, $D_s^* \bar{D}_s$, $D_s^* \bar{D}_s^*$, and so on. These decay modes can provide valuable information when searching for possible hidden-charm hadronic molecular states with hidden strangeness experimentally.

Considering the experimental potential, we strongly suggest that the BESIII Collaboration should focus on

the predicted vector hidden-charm and hidden-strange molecular state by the accumulated data from e^+e^- collision with $\sqrt{s} > 4.5$ GeV. And, the remaining three molecular states with $J^{PC} = 0^{--}, 0^{-+}, 1^{-+}$ predicted in this work can be accessible at the LHCb and BelleII by B meson decays. Additionally, theoretical study of this new type of hadronic molecular state by other approaches is also encouraged. We believe that these investigations will make our knowledge of exotic hadronic molecular states become more abundant.

ACKNOWLEDGMENTS

This work is supported by the China National Funds for Distinguished Young Scientists under Grant No. 11825503 and by the National Program for Support of Top-notch Young Professionals.

APPENDIX A: THE EFFECTIVE LAGRANGIANS

The expanded effective Lagrangians for depicting the interactions of the (anti-)charmed mesons with the light mesons are expressed as

$$\begin{aligned} \mathcal{L}_{HH\mathbb{P}} = & -\frac{2ig}{f_\pi} v^\alpha \varepsilon_{\alpha\mu\nu\lambda} D_b^{*\mu} D_a^{*\lambda\dagger} \partial^\nu \mathbb{P}_{ba} - \frac{2g}{f_\pi} (D_b^{*\mu} D_a^\dagger + D_b D_a^{*\mu\dagger}) \partial_\mu \mathbb{P}_{ba} + \frac{2ig}{f_\pi} v^\alpha \varepsilon_{\alpha\mu\nu\lambda} \bar{D}_a^{*\mu\dagger} \bar{D}_b^{*\lambda} \partial^\nu \mathbb{P}_{ab} \\ & + \frac{2g}{f_\pi} (\bar{D}_a^{*\mu\dagger} \bar{D}_b + \bar{D}_a^\dagger \bar{D}_b^{*\mu}) \partial_\mu \mathbb{P}_{ab}, \end{aligned} \quad (\text{A1})$$

$$\begin{aligned} \mathcal{L}_{HHV} = & -\sqrt{2}\beta g_V D_b D_a^\dagger v \cdot \mathbb{V}_{ba} + \sqrt{2}\beta g_V D_b^* D_a^{*\mu\dagger} v \cdot \mathbb{V}_{ba} - 2\sqrt{2}i\lambda g_V D_b^{*\mu} D_a^{*\nu\dagger} (\partial_\mu \mathbb{V}_\nu - \partial_\nu \mathbb{V}_\mu)_{ba} \\ & - 2\sqrt{2}\lambda g_V v^\lambda \varepsilon_{\lambda\mu\alpha\beta} (D_b D_a^{*\mu\dagger} + D_b^* D_a^{*\mu\dagger}) \partial^\alpha \mathbb{V}_{ba} + \sqrt{2}\beta g_V \bar{D}_a \bar{D}_b^\dagger v \cdot \mathbb{V}_{ab} - \sqrt{2}\beta g_V \bar{D}_a^* \bar{D}_b^{*\mu\dagger} v \cdot \mathbb{V}_{ab} \\ & - 2\sqrt{2}i\lambda g_V \bar{D}_a^{*\mu\dagger} \bar{D}_b^{*\nu} (\partial_\mu \mathbb{V}_\nu - \partial_\nu \mathbb{V}_\mu)_{ab} - 2\sqrt{2}\lambda g_V v^\lambda \varepsilon_{\lambda\mu\alpha\beta} (\bar{D}_a^{*\mu\dagger} \bar{D}_b + \bar{D}_a^\dagger \bar{D}_b^{*\mu}) \partial^\alpha \mathbb{V}_{ab}, \end{aligned} \quad (\text{A2})$$

$$\begin{aligned} \mathcal{L}_{TT\mathbb{P}} = & -\frac{5ik}{3f_\pi} \varepsilon^{\mu\nu\rho\tau} v_\tau D_{1b\mu}^\dagger D_{1a\nu} \partial_\rho \mathbb{P}_{ba} + \frac{2ik}{f_\pi} \varepsilon^{\mu\nu\rho\tau} v_\nu D_{2b\rho}^{*\alpha\dagger} D_{2a\alpha\tau}^* \partial_\mu \mathbb{P}_{ba} - \sqrt{\frac{2}{3}} \frac{k}{f_\pi} (D_{2b}^{*\mu\lambda} D_{1a\mu}^\dagger + D_{1b\mu} D_{2a}^{*\mu\lambda\dagger}) \partial_\lambda \mathbb{P}_{ba} \\ & - \frac{5ik}{3f_\pi} \varepsilon^{\mu\nu\rho\tau} v_\nu \bar{D}_{1a\rho}^\dagger \bar{D}_{1b\tau} \partial_\mu \mathbb{P}_{ab} + \frac{2ik}{f_\pi} \varepsilon^{\mu\nu\rho\tau} v_\nu \bar{D}_{2a\rho}^{*\alpha\dagger} \bar{D}_{2b\alpha\tau}^* \partial_\mu \mathbb{P}_{ab} + \sqrt{\frac{2}{3}} \frac{k}{f_\pi} (\bar{D}_{2a}^{*\mu\lambda} \bar{D}_{1b\mu}^\dagger + \bar{D}_{1a\mu} \bar{D}_{2b}^{*\mu\lambda\dagger}) \partial_\lambda \mathbb{P}_{ab}, \end{aligned} \quad (\text{A3})$$

$$\begin{aligned} \mathcal{L}_{TTV} = & -\sqrt{2}\beta'' g_V (v \cdot \mathbb{V}_{ba}) D_{1b\mu} D_{1a}^{\mu\dagger} + \frac{5\sqrt{2}i\lambda'' g_V}{3} (D_{1b}^\nu D_{1a}^\mu - D_{1b}^\nu D_{1a}^{\mu\dagger}) \partial_\mu \mathbb{V}_{bav} + \sqrt{2}\beta'' g_V (v \cdot \mathbb{V}_{ba}) D_{2b}^{*\lambda\nu} D_{2a\lambda\nu}^{\dagger*} \\ & + 2\sqrt{2}i\lambda'' g_V \times (D_{2b}^{*\lambda\nu} D_{2a\lambda}^{\mu\dagger} - D_{2a}^{*\lambda\nu\dagger} D_{2b\lambda}^{\mu*}) \partial_\mu \mathbb{V}_{bav} + \frac{i\beta'' g_V}{\sqrt{3}} \varepsilon^{\lambda\alpha\rho\tau} v_\rho (v \cdot \mathbb{V}_{ba}) (D_{1b\alpha}^\dagger D_{2a\lambda\tau}^* - D_{1b\alpha} D_{2a\lambda\tau}^{\dagger*}) \\ & + \frac{2\lambda'' g_V}{\sqrt{3}} [3\varepsilon^{\mu\lambda\nu\tau} v_\lambda (D_{1a}^{\alpha\dagger} D_{2b\alpha\tau}^* + D_{1b}^\alpha D_{2a\alpha\tau}^{\dagger*}) \partial_\mu \mathbb{V}_{bav} + 2\varepsilon^{\lambda\alpha\rho\nu} v_\rho (D_{1b\alpha}^\dagger D_{2a\lambda}^{\mu*} + D_{1b\alpha} D_{2a\lambda}^{\dagger*\mu}) \times (\partial_\mu \mathbb{V}_\nu - \partial_\nu \mathbb{V}_\mu)_{ba}] \\ & + \sqrt{2}\beta'' g_V (v \cdot \mathbb{V}_{ab}) \bar{D}_{1a\mu} \bar{D}_{1b}^{\mu\dagger} + \frac{5\sqrt{2}i\lambda'' g_V}{3} (\bar{D}_{1a}^\nu \bar{D}_{1b}^{\mu\dagger} - \bar{D}_{1a}^{\nu\dagger} \bar{D}_{1b}^\mu) \partial_\mu \mathbb{V}_{abv} - \sqrt{2}\beta'' g_V (v \cdot \mathbb{V}_{ab}) \bar{D}_{2a}^{*\lambda\nu} \bar{D}_{2b\lambda\nu}^{\dagger*} \\ & + 2\sqrt{2}i\lambda'' g_V (\bar{D}_{2a}^{*\lambda\nu\dagger} \bar{D}_{2b\lambda}^{\mu*} - \bar{D}_{2a}^{*\lambda\nu} \bar{D}_{2b\lambda}^{\mu\dagger}) \partial_\mu \mathbb{V}_{abv} + \frac{i\beta'' g_V}{\sqrt{3}} \varepsilon^{\lambda\alpha\rho\tau} v_\rho (v \cdot \mathbb{V}_{ba}) (\bar{D}_{1a\alpha}^\dagger \bar{D}_{2b\lambda\tau}^* - \bar{D}_{1a\alpha} \bar{D}_{2b\lambda\tau}^{\dagger*}) \\ & + \frac{2\lambda'' g_V}{\sqrt{3}} [3\varepsilon^{\mu\lambda\nu\tau} v_\lambda (\bar{D}_{1a}^{\alpha\dagger} \bar{D}_{2b\alpha\tau}^* + \bar{D}_{1a}^\alpha \bar{D}_{2b\alpha\tau}^{\dagger*}) \partial_\mu \mathbb{V}_{abv} + 2\varepsilon^{\lambda\alpha\rho\nu} v_\rho (\bar{D}_{1a\alpha}^\dagger \bar{D}_{2b\lambda}^{\mu*} + \bar{D}_{1a\alpha} \bar{D}_{2b\lambda}^{\dagger*\mu}) \times (\partial_\mu \mathbb{V}_\nu - \partial_\nu \mathbb{V}_\mu)_{ab}], \end{aligned} \quad (\text{A4})$$

$$\begin{aligned}
\mathcal{L}_{HT\mathbb{P}} = & -\frac{2h'}{f_\pi}(D_b D_{2a}^{*\mu\nu\dagger} + D_{2b}^{*\mu\nu} D_a^\dagger)\partial_\mu\partial_\nu\mathbb{P}_{ba} \\
& -\frac{\sqrt{2}h'}{\sqrt{3}f_\pi}[3(D_b^{*\mu} D_{1a}^{\nu\dagger} + D_{1b}^\nu D_a^{*\mu\dagger})\partial_\mu\partial_\nu\mathbb{P}_{ba} + (D_{\lambda b}^* D_{1a}^{\lambda\dagger} + D_{1b}^\lambda D_{\lambda a}^{*\dagger})(\partial_\nu\partial^\nu - v^\mu v^\nu\partial_\mu\partial_\nu)\mathbb{P}_{ba}] \\
& -\frac{2ih'}{f_\pi}\varepsilon^{\lambda\nu\rho\tau}v_\lambda(D_{b\tau}^* D_{2a\rho}^{*\mu\dagger} - D_{2b\rho}^{*\mu} D_{a\tau}^{*\dagger})\partial_\mu\partial_\nu\mathbb{P}_{ba} + \frac{2h'}{f_\pi}(\bar{D}_a \bar{D}_{2b}^{*\mu\nu\dagger} + \bar{D}_{2a}^{*\mu\nu} \bar{D}_b^\dagger)\partial_\mu\partial_\nu\mathbb{P}_{ab} \\
& +\frac{\sqrt{2}h'}{\sqrt{3}f_\pi}[3(\bar{D}_a^{*\mu} \bar{D}_{1b}^{\nu\dagger} + \bar{D}_{1a}^\nu \bar{D}_b^{*\mu\dagger})\partial_\mu\partial_\nu\mathbb{P}_{ab} + (\bar{D}_{\lambda a}^* \bar{D}_{1b}^{\lambda\dagger} + \bar{D}_{1a}^\lambda \bar{D}_{\lambda b}^{*\dagger})(\partial_\nu\partial^\nu - v^\mu v^\nu\partial_\mu\partial_\nu)\mathbb{P}_{ab}] \\
& -\frac{2ih'}{f_\pi}\varepsilon^{\lambda\nu\rho\tau}v_\lambda(\bar{D}_{2a\tau}^{*\mu\dagger} \bar{D}_{b\nu}^* - \bar{D}_{a\nu}^{*\dagger} \bar{D}_{2b\tau}^{*\mu})\partial_\mu\partial_\rho\mathbb{P}_{ab}, \tag{A5}
\end{aligned}$$

$$\begin{aligned}
\mathcal{L}_{HT\mathbb{V}} = & -\frac{2}{\sqrt{3}}\zeta_{1g_V}(D_b D_{1a\mu}^\dagger + D_{1b\mu} D_a^\dagger)\mathbb{V}_{ba}^\mu + \frac{2i}{\sqrt{3}}\mu_{1g_V}[(D_b D_{1a}^{\nu\dagger} - D_{1b\nu} D_a^\dagger)v^\mu(\partial_\mu\mathbb{V}_\nu - \partial_\nu\mathbb{V}_\mu)_{ba}] \\
& +\frac{i}{\sqrt{3}}\zeta_{1g_V}\varepsilon^{\mu\nu\rho\tau}v_\nu(D_{1b\mu}^\dagger D_{a\tau}^* - D_{b\tau}^{*\dagger} D_{1a\mu})\mathbb{V}_{ba\rho} + \frac{\mu_{1g_V}}{\sqrt{3}}[\varepsilon^{\alpha\beta\rho\tau}v_\beta v^\mu(D_{1b\alpha}^\dagger D_{a\tau}^* + D_{b\tau}^{*\dagger} D_{1a\alpha})\partial_\mu\mathbb{V}_{ba\rho} \\
& -\varepsilon^{\mu\beta\lambda\tau}v_\lambda v^\rho(D_{1b\beta}^\dagger D_{a\tau}^* + D_{b\tau}^{*\dagger} D_{1a\beta})\partial_\mu\mathbb{V}_{ba\rho}] + \sqrt{2}\zeta_{1g_V}(D_{2b\mu\nu}^{*\dagger} D_a^{*\mu} + D_b^{*\mu\dagger} D_{2a\mu\nu}^*)\mathbb{V}_{ba}^\nu \\
& +\sqrt{2}i\mu_{1g_V}[v_\nu(D_{2b\lambda\mu}^{*\dagger} D_a^{*\lambda} - D_b^{*\lambda\dagger} D_{2a\lambda\mu}^*) + v_\mu(D_{2b\lambda\nu}^* D_a^{*\lambda\dagger} - D_b^{*\lambda} D_{2a\lambda\nu}^{*\dagger})]\partial_\mu\mathbb{V}_{ba}^\nu \\
& +\frac{2}{\sqrt{3}}\zeta_{1g_V}(\bar{D}_a \bar{D}_{1b\mu}^\dagger + \bar{D}_{1a\mu} \bar{D}_b^\dagger)\mathbb{V}_{ab}^\mu - \frac{2i}{\sqrt{3}}\mu_{1g_V}[(\bar{D}_a \bar{D}_{1b}^{\nu\dagger} - \bar{D}_{1a\nu} \bar{D}_b^\dagger)v^\mu(\partial_\mu\mathbb{V}_\nu - \partial_\nu\mathbb{V}_\mu)_{ab}] \\
& +\frac{i}{\sqrt{3}}\zeta_{1g_V}\varepsilon^{\mu\nu\rho\tau}v_\mu(\bar{D}_{1a\rho}^\dagger \bar{D}_{b\tau}^* - \bar{D}_{a\tau}^{*\dagger} \bar{D}_{1b\rho})\mathbb{V}_{ab\nu} + \frac{\mu_{1g_V}}{\sqrt{3}}[\varepsilon^{\alpha\beta\rho\tau}v_\alpha v^\mu(\bar{D}_{1a\beta}^\dagger \bar{D}_{b\rho}^* + \bar{D}_{a\rho}^{*\dagger} \bar{D}_{1b\beta})\partial_\mu\mathbb{V}_{ab\tau} \\
& +\varepsilon^{\mu\beta\lambda\rho}v_\beta v^\tau(\bar{D}_{1a\lambda}^\dagger \bar{D}_{b\rho}^* + \bar{D}_{a\rho}^{*\dagger} \bar{D}_{1b\lambda})\partial_\mu\mathbb{V}_{ab\tau}] - \sqrt{2}\zeta_{1g_V}(\bar{D}_{2a\mu\nu}^{*\dagger} \bar{D}_b^{*\mu} + \bar{D}_a^{*\mu\dagger} \bar{D}_{2b\mu\nu}^*)\mathbb{V}_{ab}^\nu \\
& -\sqrt{2}i\mu_{1g_V}[v_\nu(\bar{D}_{2a\lambda\mu}^{*\dagger} \bar{D}_b^{*\lambda} - \bar{D}_a^{*\lambda\dagger} \bar{D}_{2b\lambda\mu}^*) + v_\mu(\bar{D}_{2a\lambda\nu}^* \bar{D}_b^{*\lambda\dagger} - \bar{D}_a^{*\lambda} \bar{D}_{2b\lambda\nu}^{*\dagger})]\partial_\mu\mathbb{V}_{ab}^\nu. \tag{A6}
\end{aligned}$$

APPENDIX B: THE DETAILS OF THESE OBTAINED EFFECTIVE POTENTIALS

Before presenting the effective potentials, we first focus on several typical Fourier transforms, i.e.,

$$\mathcal{F}\left\{\frac{1}{q^2 + m^2}\left(\frac{\Lambda^2 - m^2}{\Lambda^2 + q^2}\right)^2\right\} = Y(\Lambda, m, r), \tag{B1}$$

$$\mathcal{F}\left\{\frac{q^2}{q^2 + m^2}\left(\frac{\Lambda^2 - m^2}{\Lambda^2 + q^2}\right)^2\right\} = -ZY(\Lambda, m, r), \tag{B2}$$

$$\mathcal{F}\left\{\frac{(\mathbf{a} \cdot \mathbf{q})(\mathbf{b} \cdot \mathbf{q})}{q^2 + m^2}\left(\frac{\Lambda^2 - m^2}{\Lambda^2 + q^2}\right)^2\right\} = -\frac{1}{3}(\mathbf{a} \cdot \mathbf{b})ZY(\Lambda, m, r) - \frac{1}{3}T(\mathbf{a}, \mathbf{b})TY(\Lambda, m, r), \tag{B3}$$

$$\mathcal{F}\left\{\frac{(\mathbf{a} \times \mathbf{q}) \cdot (\mathbf{b} \times \mathbf{q})}{q^2 + m^2}\left(\frac{\Lambda^2 - m^2}{\Lambda^2 + q^2}\right)^2\right\} = -\frac{2}{3}(\mathbf{a} \cdot \mathbf{b})ZY(\Lambda, m, r) + \frac{1}{3}T(\mathbf{a}, \mathbf{b})TY(\Lambda, m, r), \tag{B4}$$

$$\begin{aligned}
\mathcal{F}\left\{\frac{(\mathbf{a} \cdot \mathbf{q})(\mathbf{b} \cdot \mathbf{q})(\mathbf{c} \cdot \mathbf{q})(\mathbf{d} \cdot \mathbf{q})}{q^2 + m^2}\left(\frac{\Lambda^2 - m^2}{\Lambda^2 + q^2}\right)^2\right\} = & \frac{1}{27}[(\mathbf{a} \cdot \mathbf{b})(\mathbf{c} \cdot \mathbf{d}) + (\mathbf{a} \cdot \mathbf{c})(\mathbf{b} \cdot \mathbf{d}) + (\mathbf{a} \cdot \mathbf{d})(\mathbf{b} \cdot \mathbf{c})]ZY(\Lambda, m, r) \\
& +\frac{1}{27}[T(\mathbf{a}, \mathbf{b})T(\mathbf{c}, \mathbf{d}) + T(\mathbf{a}, \mathbf{c})T(\mathbf{b}, \mathbf{d}) + T(\mathbf{a}, \mathbf{d})T(\mathbf{b}, \mathbf{c})]TTY(\Lambda, m, r) \\
& +\frac{1}{54}[(\mathbf{a} \cdot \mathbf{b})T(\mathbf{c}, \mathbf{d}) + (\mathbf{a} \cdot \mathbf{c})T(\mathbf{b}, \mathbf{d}) + (\mathbf{a} \cdot \mathbf{d})T(\mathbf{b}, \mathbf{c}) + (\mathbf{c} \cdot \mathbf{d})T(\mathbf{a}, \mathbf{b}) \\
& + (\mathbf{b} \cdot \mathbf{d})T(\mathbf{a}, \mathbf{c}) + (\mathbf{b} \cdot \mathbf{c})T(\mathbf{a}, \mathbf{d})]\{T, Z\}Y(\Lambda, m, r). \tag{B5}
\end{aligned}$$

In the above expressions, the operators are defined as $\mathcal{Z} = \frac{1}{r^2} \frac{\partial}{\partial r} r^2 \frac{\partial}{\partial r}$, $\mathcal{T} = r \frac{\partial}{\partial r} \frac{1}{r} \frac{\partial}{\partial r}$, $\{\mathcal{T}, \mathcal{Z}\} = \mathcal{T}\mathcal{Z} + \mathcal{Z}\mathcal{T}$, and $T(\mathbf{a}, \mathbf{b}) = 3(\hat{\mathbf{r}} \cdot \mathbf{a})(\hat{\mathbf{r}} \cdot \mathbf{b}) - \mathbf{a} \cdot \mathbf{b}$.

Through the above preparation, we can write out the effective potentials in the coordinate space for all of the investigated systems, which include

(i) $D_s \bar{D}_{s1} \rightarrow D_s \bar{D}_{s1}$ process:

$$\mathcal{V}_D = \frac{C}{2} \frac{\mathcal{A}_1 + \mathcal{A}'_1}{2} Y_\phi, \quad (\text{B6})$$

$$\mathcal{V}_C = \frac{E}{3} \frac{\mathcal{A}_2 + \mathcal{A}'_2}{2} Y_{\phi 0}. \quad (\text{B7})$$

(ii) $D_s \bar{D}_{s2}^* \rightarrow D_s \bar{D}_{s2}^*$ process:

$$\mathcal{V}_D = \frac{C}{2} \frac{\mathcal{A}_3 + \mathcal{A}'_3}{2} Y_\phi, \quad (\text{B8})$$

$$\mathcal{V}_C = \frac{2B}{3} \left[\frac{\mathcal{A}_4 + \mathcal{A}'_4}{2} \mathcal{Z}\mathcal{Z} + \frac{\mathcal{A}_5 + \mathcal{A}'_5}{2} \mathcal{T}\mathcal{T} + \frac{\mathcal{A}_6 + \mathcal{A}'_6}{2} \{\mathcal{T}, \mathcal{Z}\} \right] Y_{\eta 1}. \quad (\text{B9})$$

(iii) $D_s^* \bar{D}_{s1} \rightarrow D_s^* \bar{D}_{s1}$ process:

$$\mathcal{V}_D = \frac{5A}{27} [\mathcal{A}_8 \mathcal{Z} + \mathcal{A}_9 \mathcal{T}] Y_\eta + \left[\frac{C}{2} \mathcal{A}_7 + \frac{5D}{9} (\mathcal{A}_9 \mathcal{T} - 2\mathcal{A}_8 \mathcal{Z}) \right] Y_\phi, \quad (\text{B10})$$

$$\mathcal{V}_C = \frac{B}{9} [\mathcal{A}_{10} \mathcal{Z}\mathcal{Z} + \mathcal{A}_{11} \mathcal{T}\mathcal{T} + \mathcal{A}_{12} \{\mathcal{T}, \mathcal{Z}\}] Y_{\eta 2} + \frac{E}{12} \mathcal{A}_8 Y_{\phi 2}. \quad (\text{B11})$$

(iv) $D_s^* \bar{D}_{s2}^* \rightarrow D_s^* \bar{D}_{s2}^*$ process:

$$\begin{aligned} \mathcal{V}_D = & \frac{2A}{9} \left[\frac{\mathcal{A}_{14} + \mathcal{A}'_{14}}{2} \mathcal{Z} + \frac{\mathcal{A}_{15} + \mathcal{A}'_{15}}{2} \mathcal{T} \right] Y_\eta \\ & + \left[\frac{2D}{3} \left(\frac{\mathcal{A}_{15} + \mathcal{A}'_{15}}{2} \mathcal{T} - 2 \frac{\mathcal{A}_{14} + \mathcal{A}'_{14}}{2} \mathcal{Z} \right) + \frac{C}{2} \frac{\mathcal{A}_{13} + \mathcal{A}'_{13}}{2} \right] Y_\phi, \end{aligned} \quad (\text{B12})$$

$$\mathcal{V}_C = \frac{2B}{3} \left[\frac{\mathcal{A}_{16} + \mathcal{A}'_{16}}{2} \mathcal{Z}\mathcal{Z} + \frac{\mathcal{A}_{17} + \mathcal{A}'_{17}}{2} \mathcal{T}\mathcal{T} + \frac{\mathcal{A}_{18} + \mathcal{A}'_{18}}{2} \{\mathcal{T}, \mathcal{Z}\} \right] Y_{\eta 3} + \frac{E}{2} \frac{\mathcal{A}_{19} + \mathcal{A}'_{19}}{2} Y_{\phi 3}. \quad (\text{B13})$$

Here, $A = gk/f_\pi^2$, $B = h^2/f_\pi^2$, $C = \beta\beta'' g_V^2$, $D = \lambda\lambda'' g_V^2$, and $E = \zeta_1^2 g_V^2$. In the above expressions, the function $Y(\Lambda_i, m_i, r)$ reads as

$$Y_i \equiv Y(\Lambda_i, m_i, r) = \frac{e^{-m_i r} - e^{-\Lambda_i r}}{4\pi r} - \frac{\Lambda_i^2 - m_i^2}{8\pi\Lambda_i} e^{-\Lambda_i r} \quad (\text{B14})$$

with $m_i = \sqrt{m^2 - q_i^2}$ and $\Lambda_i = \sqrt{\Lambda^2 - q_i^2}$. The variables q_i are defined as $q_0 = m_{D_{s1}} - m_{D_s}$, $q_1 = m_{D_{s2}^*} - m_{D_s}$, $q_2 = m_{D_{s1}} - m_{D_s^*}$, and $q_3 = m_{D_{s2}^*} - m_{D_s^*}$. In addition, we introduce several operators, which include

$$\begin{aligned}
\mathcal{A}_1 &= \boldsymbol{\epsilon}_4^\dagger \cdot \boldsymbol{\epsilon}_2, & \mathcal{A}'_1 &= \boldsymbol{\epsilon}_3^\dagger \cdot \boldsymbol{\epsilon}_1, & \mathcal{A}_2 &= \boldsymbol{\epsilon}_3^\dagger \cdot \boldsymbol{\epsilon}_2, & \mathcal{A}'_2 &= \boldsymbol{\epsilon}_4^\dagger \cdot \boldsymbol{\epsilon}_1, \\
\mathcal{A}_3 &= \sum (\boldsymbol{\epsilon}_{4m}^\dagger \cdot \boldsymbol{\epsilon}_{2a})(\boldsymbol{\epsilon}_{4n}^\dagger \cdot \boldsymbol{\epsilon}_{2b}), & \mathcal{A}'_3 &= \sum (\boldsymbol{\epsilon}_{3m}^\dagger \cdot \boldsymbol{\epsilon}_{1a})(\boldsymbol{\epsilon}_{3n}^\dagger \cdot \boldsymbol{\epsilon}_{1b}), \\
\mathcal{A}_4 &= \frac{2}{27} \sum (\boldsymbol{\epsilon}_{3m}^\dagger \cdot \boldsymbol{\epsilon}_{2a})(\boldsymbol{\epsilon}_{3n}^\dagger \cdot \boldsymbol{\epsilon}_{2b}), & \mathcal{A}'_4 &= \frac{2}{27} \sum (\boldsymbol{\epsilon}_{4m}^\dagger \cdot \boldsymbol{\epsilon}_{1a})(\boldsymbol{\epsilon}_{4n}^\dagger \cdot \boldsymbol{\epsilon}_{1b}), \\
\mathcal{A}_5 &= \frac{1}{27} \sum T(\boldsymbol{\epsilon}_{3m}^\dagger, \boldsymbol{\epsilon}_{3n}^\dagger)T(\boldsymbol{\epsilon}_{2a}, \boldsymbol{\epsilon}_{2b}) + \frac{2}{27} \sum T(\boldsymbol{\epsilon}_{3m}^\dagger, \boldsymbol{\epsilon}_{2a})T(\boldsymbol{\epsilon}_{3n}^\dagger, \boldsymbol{\epsilon}_{2b}), \\
\mathcal{A}'_5 &= \frac{1}{27} \sum T(\boldsymbol{\epsilon}_{4m}^\dagger, \boldsymbol{\epsilon}_{4n}^\dagger)T(\boldsymbol{\epsilon}_{1a}, \boldsymbol{\epsilon}_{1b}) + \frac{2}{27} \sum T(\boldsymbol{\epsilon}_{4m}^\dagger, \boldsymbol{\epsilon}_{1a})T(\boldsymbol{\epsilon}_{4n}^\dagger, \boldsymbol{\epsilon}_{1b}), \\
\mathcal{A}_6 &= \frac{2}{27} \sum (\boldsymbol{\epsilon}_{3m}^\dagger \cdot \boldsymbol{\epsilon}_{2a})T(\boldsymbol{\epsilon}_{3n}^\dagger, \boldsymbol{\epsilon}_{2b}), & \mathcal{A}'_6 &= \frac{2}{27} \sum (\boldsymbol{\epsilon}_{4m}^\dagger \cdot \boldsymbol{\epsilon}_{1a})T(\boldsymbol{\epsilon}_{4n}^\dagger, \boldsymbol{\epsilon}_{1b}), \\
\mathcal{A}_7 &= (\boldsymbol{\epsilon}_3^\dagger \cdot \boldsymbol{\epsilon}_1)(\boldsymbol{\epsilon}_4^\dagger \cdot \boldsymbol{\epsilon}_2), & \mathcal{A}_8 &= (\boldsymbol{\epsilon}_3^\dagger \times \boldsymbol{\epsilon}_1) \cdot (\boldsymbol{\epsilon}_4^\dagger \times \boldsymbol{\epsilon}_2), & \mathcal{A}_9 &= T(\boldsymbol{\epsilon}_3^\dagger \times \boldsymbol{\epsilon}_1, \boldsymbol{\epsilon}_4^\dagger \times \boldsymbol{\epsilon}_2), \\
\mathcal{A}_{10} &= -\frac{1}{3}(\boldsymbol{\epsilon}_3^\dagger \cdot \boldsymbol{\epsilon}_1)(\boldsymbol{\epsilon}_4^\dagger \cdot \boldsymbol{\epsilon}_2) + \frac{1}{3}(\boldsymbol{\epsilon}_3^\dagger \cdot \boldsymbol{\epsilon}_4^\dagger)(\boldsymbol{\epsilon}_1 \cdot \boldsymbol{\epsilon}_2), & \mathcal{A}_{11} &= \frac{2}{3}T(\boldsymbol{\epsilon}_3^\dagger, \boldsymbol{\epsilon}_1)T(\boldsymbol{\epsilon}_4^\dagger, \boldsymbol{\epsilon}_2) + \frac{1}{3}T(\boldsymbol{\epsilon}_3^\dagger, \boldsymbol{\epsilon}_4^\dagger)T(\boldsymbol{\epsilon}_1, \boldsymbol{\epsilon}_2), \\
\mathcal{A}_{12} &= \frac{1}{6}(\boldsymbol{\epsilon}_3^\dagger \cdot \boldsymbol{\epsilon}_4^\dagger)T(\boldsymbol{\epsilon}_1, \boldsymbol{\epsilon}_2) + \frac{1}{6}(\boldsymbol{\epsilon}_1 \cdot \boldsymbol{\epsilon}_2)T(\boldsymbol{\epsilon}_3^\dagger, \boldsymbol{\epsilon}_4^\dagger) - \frac{1}{3}(\boldsymbol{\epsilon}_3^\dagger \cdot \boldsymbol{\epsilon}_1)T(\boldsymbol{\epsilon}_4^\dagger, \boldsymbol{\epsilon}_2), \\
\mathcal{A}_{13} &= \sum (\boldsymbol{\epsilon}_3^\dagger \cdot \boldsymbol{\epsilon}_1)(\boldsymbol{\epsilon}_{4m}^\dagger \cdot \boldsymbol{\epsilon}_{2a})(\boldsymbol{\epsilon}_{4n}^\dagger \cdot \boldsymbol{\epsilon}_{2b}), & \mathcal{A}'_{13} &= \sum (\boldsymbol{\epsilon}_4^\dagger \cdot \boldsymbol{\epsilon}_2)(\boldsymbol{\epsilon}_{3m}^\dagger \cdot \boldsymbol{\epsilon}_{1a})(\boldsymbol{\epsilon}_{3n}^\dagger \cdot \boldsymbol{\epsilon}_{1b}), \\
\mathcal{A}_{14} &= \sum (\boldsymbol{\epsilon}_{4m}^\dagger \cdot \boldsymbol{\epsilon}_{2a})[(\boldsymbol{\epsilon}_3^\dagger \times \boldsymbol{\epsilon}_1) \cdot (\boldsymbol{\epsilon}_{4n}^\dagger \times \boldsymbol{\epsilon}_{2b})], & \mathcal{A}'_{14} &= \sum (\boldsymbol{\epsilon}_{3m}^\dagger \cdot \boldsymbol{\epsilon}_{1a})[(\boldsymbol{\epsilon}_4^\dagger \times \boldsymbol{\epsilon}_2) \cdot (\boldsymbol{\epsilon}_{3n}^\dagger \times \boldsymbol{\epsilon}_{1b})], \\
\mathcal{A}_{15} &= \sum (\boldsymbol{\epsilon}_{4m}^\dagger \cdot \boldsymbol{\epsilon}_{2a})T(\boldsymbol{\epsilon}_3^\dagger \times \boldsymbol{\epsilon}_1, \boldsymbol{\epsilon}_{4n}^\dagger \times \boldsymbol{\epsilon}_{2b}), & \mathcal{A}'_{15} &= \sum (\boldsymbol{\epsilon}_{3m}^\dagger \cdot \boldsymbol{\epsilon}_{1a})T(\boldsymbol{\epsilon}_4^\dagger \times \boldsymbol{\epsilon}_2, \boldsymbol{\epsilon}_{3n}^\dagger \times \boldsymbol{\epsilon}_{1b}), \\
\mathcal{A}_{16} &= \frac{1}{27} \sum [(\boldsymbol{\epsilon}_{3m}^\dagger \times \boldsymbol{\epsilon}_1) \cdot (\boldsymbol{\epsilon}_4^\dagger \times \boldsymbol{\epsilon}_{2a})](\boldsymbol{\epsilon}_{3n}^\dagger \cdot \boldsymbol{\epsilon}_{2b}) + \frac{1}{27} \sum [(\boldsymbol{\epsilon}_{3m}^\dagger \times \boldsymbol{\epsilon}_1) \cdot \boldsymbol{\epsilon}_{2b}][\boldsymbol{\epsilon}_{3n}^\dagger \cdot (\boldsymbol{\epsilon}_4^\dagger \times \boldsymbol{\epsilon}_{2a})], \\
\mathcal{A}'_{16} &= \frac{1}{27} \sum [(\boldsymbol{\epsilon}_{4m}^\dagger \times \boldsymbol{\epsilon}_2) \cdot (\boldsymbol{\epsilon}_3^\dagger \times \boldsymbol{\epsilon}_{1a})](\boldsymbol{\epsilon}_{4n}^\dagger \cdot \boldsymbol{\epsilon}_{1b}) + \frac{1}{27} \sum [(\boldsymbol{\epsilon}_{4m}^\dagger \times \boldsymbol{\epsilon}_2) \cdot \boldsymbol{\epsilon}_{1b}][\boldsymbol{\epsilon}_{4n}^\dagger \cdot (\boldsymbol{\epsilon}_3^\dagger \times \boldsymbol{\epsilon}_{1a})], \\
\mathcal{A}_{17} &= \frac{1}{27} \sum T(\boldsymbol{\epsilon}_{3m}^\dagger \times \boldsymbol{\epsilon}_1, \boldsymbol{\epsilon}_{3n}^\dagger)T(\boldsymbol{\epsilon}_4^\dagger \times \boldsymbol{\epsilon}_{2a}, \boldsymbol{\epsilon}_{2b}) + \frac{1}{27} \sum T(\boldsymbol{\epsilon}_{3m}^\dagger \times \boldsymbol{\epsilon}_1, \boldsymbol{\epsilon}_4^\dagger \times \boldsymbol{\epsilon}_{2a})T(\boldsymbol{\epsilon}_{3n}^\dagger, \boldsymbol{\epsilon}_{2b}) \\
&\quad + \frac{1}{27} \sum T(\boldsymbol{\epsilon}_{3m}^\dagger \times \boldsymbol{\epsilon}_1, \boldsymbol{\epsilon}_{2b})T(\boldsymbol{\epsilon}_{3n}^\dagger, \boldsymbol{\epsilon}_4^\dagger \times \boldsymbol{\epsilon}_{2a}), \\
\mathcal{A}'_{17} &= \frac{1}{27} \sum T(\boldsymbol{\epsilon}_{4m}^\dagger \times \boldsymbol{\epsilon}_2, \boldsymbol{\epsilon}_{4n}^\dagger)T(\boldsymbol{\epsilon}_3^\dagger \times \boldsymbol{\epsilon}_{1a}, \boldsymbol{\epsilon}_{1b}) + \frac{1}{27} \sum T(\boldsymbol{\epsilon}_{4m}^\dagger \times \boldsymbol{\epsilon}_2, \boldsymbol{\epsilon}_3^\dagger \times \boldsymbol{\epsilon}_{1a})T(\boldsymbol{\epsilon}_{4n}^\dagger, \boldsymbol{\epsilon}_{1b}) \\
&\quad + \frac{1}{27} \sum T(\boldsymbol{\epsilon}_{4m}^\dagger \times \boldsymbol{\epsilon}_2, \boldsymbol{\epsilon}_{1b})T(\boldsymbol{\epsilon}_{4n}^\dagger, \boldsymbol{\epsilon}_3^\dagger \times \boldsymbol{\epsilon}_{1a}), \\
\mathcal{A}_{18} &= \frac{1}{54} \sum [(\boldsymbol{\epsilon}_{3m}^\dagger \times \boldsymbol{\epsilon}_1) \cdot (\boldsymbol{\epsilon}_4^\dagger \times \boldsymbol{\epsilon}_{2a})]T(\boldsymbol{\epsilon}_{3n}^\dagger, \boldsymbol{\epsilon}_{2b}) + \frac{1}{54} \sum [(\boldsymbol{\epsilon}_{3m}^\dagger \times \boldsymbol{\epsilon}_1) \cdot \boldsymbol{\epsilon}_{2b}]T(\boldsymbol{\epsilon}_{3n}^\dagger, \boldsymbol{\epsilon}_4^\dagger \times \boldsymbol{\epsilon}_{2a}) \\
&\quad + \frac{1}{54} \sum (\boldsymbol{\epsilon}_{3n}^\dagger \cdot \boldsymbol{\epsilon}_{2b})T(\boldsymbol{\epsilon}_{3m}^\dagger \times \boldsymbol{\epsilon}_1, \boldsymbol{\epsilon}_4^\dagger \times \boldsymbol{\epsilon}_{2a}) + \frac{1}{54} \sum [\boldsymbol{\epsilon}_{3n}^\dagger \cdot (\boldsymbol{\epsilon}_4^\dagger \times \boldsymbol{\epsilon}_{2a})]T(\boldsymbol{\epsilon}_{3m}^\dagger \times \boldsymbol{\epsilon}_1, \boldsymbol{\epsilon}_{2b}), \\
\mathcal{A}'_{18} &= \frac{1}{54} \sum [(\boldsymbol{\epsilon}_{4m}^\dagger \times \boldsymbol{\epsilon}_2) \cdot (\boldsymbol{\epsilon}_3^\dagger \times \boldsymbol{\epsilon}_{1a})]T(\boldsymbol{\epsilon}_{4n}^\dagger, \boldsymbol{\epsilon}_{1b}) + \frac{1}{54} \sum [(\boldsymbol{\epsilon}_{4m}^\dagger \times \boldsymbol{\epsilon}_2) \cdot \boldsymbol{\epsilon}_{1b}]T(\boldsymbol{\epsilon}_{4n}^\dagger, \boldsymbol{\epsilon}_3^\dagger \times \boldsymbol{\epsilon}_{1a}) \\
&\quad + \frac{1}{54} \sum (\boldsymbol{\epsilon}_{4n}^\dagger \cdot \boldsymbol{\epsilon}_{1b})T(\boldsymbol{\epsilon}_{4m}^\dagger \times \boldsymbol{\epsilon}_2, \boldsymbol{\epsilon}_3^\dagger \times \boldsymbol{\epsilon}_{1a}) + \frac{1}{54} \sum [\boldsymbol{\epsilon}_{4n}^\dagger \cdot (\boldsymbol{\epsilon}_3^\dagger \times \boldsymbol{\epsilon}_{1a})]T(\boldsymbol{\epsilon}_{4m}^\dagger \times \boldsymbol{\epsilon}_2, \boldsymbol{\epsilon}_{1b}), \\
\mathcal{A}_{19} &= \sum (\boldsymbol{\epsilon}_{3m}^\dagger \cdot \boldsymbol{\epsilon}_1)(\boldsymbol{\epsilon}_4^\dagger \cdot \boldsymbol{\epsilon}_{2a})(\boldsymbol{\epsilon}_{3n}^\dagger \cdot \boldsymbol{\epsilon}_{2b}), & \mathcal{A}'_{19} &= \sum (\boldsymbol{\epsilon}_{4m}^\dagger \cdot \boldsymbol{\epsilon}_2)(\boldsymbol{\epsilon}_3^\dagger \cdot \boldsymbol{\epsilon}_{1a})(\boldsymbol{\epsilon}_{4n}^\dagger \cdot \boldsymbol{\epsilon}_{1b}). \tag{B15}
\end{aligned}$$

Here, we define $\sum = \sum_{m,n,a,b} C_{1m,1n}^{2,m+n} C_{1a,1b}^{2,a+b}$. For these operators $\mathcal{A}_k^{(l)}$, they should be sandwiched by the spin-orbital wave functions $|^{2S+1}L_J\rangle$, we present the relevant operator matrix elements $\mathcal{A}_k^{(l)}[J]$ in Table X.

TABLE X. The relevant operator matrix elements $\mathcal{A}_k^{(j)}[J](k=1, \dots, 19)$ for the S -wave $H_s \bar{T}_s$ systems.

$\mathcal{A}_k^{(j)}[J] = \langle f \mathcal{A}_k^{(j)} i \rangle$		
$\mathcal{A}_1^{(0)}[1] = \text{diag}(1, 1)$	$\mathcal{A}_2^{(0)}[1] = \text{diag}(1, 1)$	$\mathcal{A}_3^{(0)}[2] = \text{diag}(1, 1)$
$\mathcal{A}_4^{(0)}[2] = \text{diag}(\frac{2}{27}, \frac{2}{27})$	$\mathcal{A}_7[0] = \text{diag}(1, 1)$	$\mathcal{A}_8[0] = \text{diag}(2, -1)$
$\mathcal{A}_{10}[0] = \text{diag}(\frac{2}{3}, -\frac{1}{3})$	$\mathcal{A}_{12}[0] = \begin{pmatrix} 0 & \frac{\sqrt{2}}{15} \\ -\frac{8\sqrt{2}}{15} & -\frac{1}{15} \end{pmatrix}$	$\mathcal{A}_{11}[1] = \begin{pmatrix} -\frac{2}{3} & -\frac{2\sqrt{2}}{3} & 0 \\ -\frac{2\sqrt{2}}{3} & 0 & 0 \\ 0 & 0 & -\frac{4}{3} \end{pmatrix}$
$\mathcal{A}_9[2] = \begin{pmatrix} 0 & \frac{\sqrt{2}}{\sqrt{5}} & 0 & -\frac{\sqrt{14}}{\sqrt{5}} \\ \frac{\sqrt{2}}{\sqrt{5}} & 0 & 0 & -\frac{2}{\sqrt{7}} \\ 0 & 0 & -1 & 0 \\ -\frac{\sqrt{14}}{\sqrt{5}} & -\frac{2}{\sqrt{7}} & 0 & -\frac{3}{7} \end{pmatrix}$	$\mathcal{A}_{13}^{(0)}[1] = \text{diag}(1, 1, 1, 1)$	$\mathcal{A}_{14}^{(0)}[1] = \text{diag}(\frac{3}{2}, \frac{3}{2}, \frac{1}{2}, -1)$
$\mathcal{A}_{15}^{(0)}[1] = \text{diag}(\frac{1}{18}, \frac{1}{18}, \frac{5}{54}, -\frac{1}{27})$	$\mathcal{A}_{16}^{(0)}[1] = \text{diag}(\frac{1}{6}, \frac{1}{6}, \frac{1}{2}, 1)$	$\mathcal{A}_{17}^{(0)}[1] = \begin{pmatrix} \frac{2}{45} & -\frac{\sqrt{2}}{45} & 0 & \frac{\sqrt{2}}{15\sqrt{21}} \\ -\frac{\sqrt{2}}{45} & \frac{1}{15} & 0 & -\frac{8}{15\sqrt{21}} \\ 0 & 0 & -\frac{9}{27\sqrt{7}} & -\frac{2\sqrt{5}}{27\sqrt{7}} \\ \frac{\sqrt{2}}{15\sqrt{21}} & -\frac{8}{15\sqrt{21}} & \frac{2\sqrt{5}}{27\sqrt{7}} & \frac{92}{945} \end{pmatrix}$
$\mathcal{A}_{18}^{(0)}[1] = \begin{pmatrix} 0 & -\frac{7}{90\sqrt{2}} & 0 & \frac{\sqrt{7}}{30\sqrt{6}} \\ -\frac{7}{90\sqrt{2}} & \frac{7}{180} & 0 & -\frac{1}{30\sqrt{21}} \\ 0 & 0 & \frac{1}{108} & -\frac{\sqrt{5}}{27\sqrt{7}} \\ \frac{\sqrt{7}}{30\sqrt{6}} & -\frac{1}{30\sqrt{21}} & \frac{\sqrt{5}}{27\sqrt{7}} & \frac{4}{315} \end{pmatrix}$	$\mathcal{A}_{19}^{(0)}[1] = \text{diag}(\frac{1}{2}, \frac{1}{2}, 1, 1)$	$\mathcal{A}_{17}^{(0)}[2] = \begin{pmatrix} 0 & \frac{3\sqrt{2}}{5} & -\frac{\sqrt{7}}{\sqrt{10}} & -\frac{\sqrt{7}}{5} \\ \frac{3\sqrt{2}}{5} & \frac{3}{10} & -\frac{3}{\sqrt{35}} & \frac{3\sqrt{2}}{5\sqrt{7}} \\ -\frac{\sqrt{7}}{\sqrt{10}} & -\frac{3}{\sqrt{35}} & -\frac{3}{14} & -\frac{4\sqrt{2}}{7\sqrt{5}} \\ -\frac{\sqrt{7}}{5} & -\frac{3\sqrt{2}}{5\sqrt{7}} & -\frac{4\sqrt{2}}{7\sqrt{5}} & \frac{12}{35} \end{pmatrix}$
$\mathcal{A}_{18}^{(0)}[2] = \begin{pmatrix} 0 & 0 & -\frac{\sqrt{7}}{54\sqrt{10}} & \frac{\sqrt{7}}{54} \\ 0 & -\frac{7}{180} & 0 & -\frac{1}{15\sqrt{14}} \\ -\frac{\sqrt{7}}{54\sqrt{10}} & 0 & -\frac{1}{252} & \frac{2\sqrt{10}}{189} \\ -\frac{\sqrt{7}}{54} & -\frac{1}{15\sqrt{14}} & -\frac{2\sqrt{10}}{189} & \frac{1}{135} \end{pmatrix}$	$\mathcal{A}_{13}^{(0)}[2] = \text{diag}(1, 1, 1, 1)$	$\mathcal{A}_{14}^{(0)}[2] = \text{diag}(\frac{1}{2}, \frac{3}{2}, \frac{1}{2}, -1)$
$\mathcal{A}_{15}^{(0)}[3] = \begin{pmatrix} 0 & \frac{3}{5\sqrt{2}} & -\frac{1}{\sqrt{5}} & -\frac{4\sqrt{3}}{5} \\ \frac{3}{5\sqrt{2}} & -\frac{3}{35} & -\frac{6\sqrt{2}}{7\sqrt{5}} & -\frac{6\sqrt{6}}{35} \\ -\frac{1}{\sqrt{5}} & -\frac{6\sqrt{2}}{7\sqrt{5}} & -\frac{4}{7} & \frac{\sqrt{3}}{7\sqrt{5}} \\ -\frac{4\sqrt{3}}{5} & -\frac{6\sqrt{6}}{35} & \frac{\sqrt{3}}{7\sqrt{5}} & -\frac{22}{35} \end{pmatrix}$	$\mathcal{A}_{16}^{(0)}[2] = \text{diag}(\frac{5}{54}, \frac{1}{18}, \frac{5}{54}, -\frac{1}{27})$	$\mathcal{A}_{19}^{(0)}[2] = \text{diag}(\frac{1}{2}, \frac{1}{2}, 1, 1)$
$\mathcal{A}_{17}^{(0)}[3] = \begin{pmatrix} 0 & \frac{2}{27} & -\frac{\sqrt{2}}{27\sqrt{35}} & \frac{2}{27\sqrt{7}} \\ 0 & \frac{1}{45} & 0 & \frac{\sqrt{2}}{15\sqrt{7}} \\ -\frac{\sqrt{2}}{27\sqrt{35}} & 0 & \frac{29}{189} & \frac{5\sqrt{10}}{189} \\ -\frac{2}{27\sqrt{7}} & \frac{\sqrt{2}}{15\sqrt{7}} & -\frac{5\sqrt{10}}{189} & -\frac{28}{135} \end{pmatrix}$	$\mathcal{A}_{17}^{(0)}[3] = \begin{pmatrix} 0 & 0 & -\frac{\sqrt{7}}{54\sqrt{10}} & -\frac{\sqrt{7}}{54} \\ 0 & -\frac{7}{180} & 0 & -\frac{1}{15\sqrt{14}} \\ -\frac{\sqrt{7}}{54\sqrt{10}} & 0 & -\frac{1}{252} & -\frac{2\sqrt{10}}{189} \\ \frac{\sqrt{7}}{54} & -\frac{1}{15\sqrt{14}} & \frac{2\sqrt{10}}{189} & \frac{1}{135} \end{pmatrix}$	$\mathcal{A}_{13}^{(0)}[3] = \text{diag}(1, 1, 1, 1)$
	$\mathcal{A}_{14}^{(0)}[3] = \text{diag}(-1, \frac{3}{2}, \frac{1}{2}, -1)$	$\mathcal{A}_{16}^{(0)}[3] = \text{diag}(-\frac{1}{27}, \frac{1}{18}, \frac{5}{54}, -\frac{1}{27})$
	$\mathcal{A}_{19}^{(0)}[3] = \text{diag}(1, \frac{1}{6}, \frac{1}{2}, 1)$	$\mathcal{A}_{17}^{(0)}[3] = \begin{pmatrix} -\frac{4}{135} & \frac{\sqrt{2}}{105} & \frac{2\sqrt{5}}{189} & -\frac{4}{315\sqrt{3}} \\ \frac{\sqrt{2}}{105} & \frac{16}{315} & 0 & -\frac{\sqrt{2}}{35\sqrt{3}} \\ -\frac{2\sqrt{5}}{189} & 0 & \frac{1}{21} & -\frac{\sqrt{5}}{63\sqrt{3}} \\ -\frac{4}{315\sqrt{3}} & -\frac{\sqrt{2}}{35\sqrt{3}} & \frac{\sqrt{5}}{63\sqrt{3}} & \frac{82}{945} \end{pmatrix}$

(Table continued)

TABLE X. (Continued)

$$\mathcal{A}_k^{(i)}[J] = \langle f | \mathcal{A}_k^{(i)} | i \rangle$$

$$\mathcal{A}'_{17}[3] = \begin{pmatrix} -\frac{4}{135} & \frac{\sqrt{2}}{105} & -\frac{2\sqrt{5}}{189} & -\frac{4}{315\sqrt{3}} \\ \frac{\sqrt{2}}{105} & \frac{16}{315} & 0 & -\frac{\sqrt{2}}{35\sqrt{3}} \\ \frac{2\sqrt{5}}{189} & 0 & \frac{1}{21} & \frac{\sqrt{5}}{63\sqrt{3}} \\ -\frac{4}{315\sqrt{3}} & -\frac{\sqrt{2}}{35\sqrt{3}} & -\frac{\sqrt{5}}{63\sqrt{3}} & \frac{82}{945} \end{pmatrix} \quad \mathcal{A}_{18}[3] = \begin{pmatrix} 0 & \frac{1}{30\sqrt{2}} & \frac{\sqrt{5}}{54} & -\frac{1}{45\sqrt{3}} \\ \frac{1}{30\sqrt{2}} & \frac{1}{90} & 0 & -\frac{\sqrt{2}}{35\sqrt{3}} \\ -\frac{\sqrt{5}}{54} & 0 & -\frac{2}{189} & \frac{\sqrt{5}}{126\sqrt{3}} \\ -\frac{1}{45\sqrt{3}} & -\frac{\sqrt{2}}{35\sqrt{3}} & -\frac{\sqrt{5}}{126\sqrt{3}} & -\frac{11}{1890} \end{pmatrix} \quad \mathcal{A}'_{18}[3] = \begin{pmatrix} 0 & \frac{1}{30\sqrt{2}} & -\frac{\sqrt{5}}{54} & -\frac{1}{45\sqrt{3}} \\ \frac{1}{30\sqrt{2}} & \frac{1}{90} & 0 & -\frac{\sqrt{2}}{35\sqrt{3}} \\ \frac{\sqrt{5}}{54} & 0 & -\frac{2}{189} & -\frac{\sqrt{5}}{126\sqrt{3}} \\ -\frac{1}{45\sqrt{3}} & -\frac{\sqrt{2}}{35\sqrt{3}} & \frac{\sqrt{5}}{126\sqrt{3}} & -\frac{11}{1890} \end{pmatrix}$$

- [1] S. K. Choi *et al.* (Belle Collaboration), Observation of a Narrow Charmonium-Like State in Exclusive $B^\pm \rightarrow K^\pm \pi^+ \pi^- J/\psi$ Decays, *Phys. Rev. Lett.* **91**, 262001 (2003).
- [2] H. X. Chen, W. Chen, X. Liu, and S. L. Zhu, The hidden-charm pentaquark and tetraquark states, *Phys. Rep.* **639**, 1 (2016).
- [3] X. Liu, An overview of XYZ new particles, *Chin. Sci. Bull.* **59**, 3815 (2014).
- [4] A. Hosaka, T. Iijima, K. Miyabayashi, Y. Sakai, and S. Yasui, Exotic hadrons with heavy flavors: X , Y , Z , and related states, *Prog. Theor. Exp. Phys.* (2016), 062C01.
- [5] Y. R. Liu, H. X. Chen, W. Chen, X. Liu, and S. L. Zhu, Pentaquark and tetraquark states, *Prog. Part. Nucl. Phys.* **107**, 237 (2019).
- [6] N. Brambilla, S. Eidelman, C. Hanhart, A. Nefediev, C. P. Shen, C. E. Thomas, A. Vairo, and C. Z. Yuan, The XYZ states: Experimental and theoretical status and perspectives, *Phys. Rep.* **873**, 1 (2020).
- [7] S. L. Olsen, T. Skwarnicki, and D. Zieminska, Nonstandard heavy mesons and baryons: Experimental evidence, *Rev. Mod. Phys.* **90**, 015003 (2018).
- [8] F. K. Guo, C. Hanhart, U. G. Meißner, Q. Wang, Q. Zhao, and B. S. Zou, Hadronic molecules, *Rev. Mod. Phys.* **90**, 015004 (2018).
- [9] R. Aaij *et al.* (LHCb Collaboration), Observation of a Narrow Pentaquark State, $P_c(4312)^+$, and of Two-Peak Structure of the $P_c(4450)^+$, *Phys. Rev. Lett.* **122**, 222001 (2019).
- [10] X. Q. Li and X. Liu, A possible global group structure for exotic states, *Eur. Phys. J. C* **74**, 3198 (2014).
- [11] M. Karliner and J. L. Rosner, New Exotic Meson and Baryon Resonances from Doubly-Heavy Hadronic Molecules, *Phys. Rev. Lett.* **115**, 122001 (2015).
- [12] J. J. Wu, R. Molina, E. Oset, and B. S. Zou, Prediction of Narrow N^* and Λ^* Resonances with Hidden Charm Above 4 GeV, *Phys. Rev. Lett.* **105**, 232001 (2010).
- [13] W. L. Wang, F. Huang, Z. Y. Zhang, and B. S. Zou, $\Sigma_c \bar{D}$ and $\Lambda_c \bar{D}$ states in a chiral quark model, *Phys. Rev. C* **84**, 015203 (2011).
- [14] Z. C. Yang, Z. F. Sun, J. He, X. Liu, and S. L. Zhu, The possible hidden-charm molecular baryons composed of anti-charmed meson and charmed baryon, *Chin. Phys. C* **36**, 6 (2012).
- [15] J. J. Wu, T.-S. H. Lee, and B. S. Zou, Nucleon resonances with hidden charm in coupled-channel models, *Phys. Rev. C* **85**, 044002 (2012).
- [16] R. Chen, X. Liu, X. Q. Li, and S. L. Zhu, Identifying Exotic Hidden-Charm Pentaquarks, *Phys. Rev. Lett.* **115**, 132002 (2015).
- [17] C. Y. Wong, Molecular states of heavy quark mesons, *Phys. Rev. C* **69**, 055202 (2004).
- [18] E. S. Swanson, Short range structure in the $X(3872)$, *Phys. Lett. B* **588**, 189 (2004).
- [19] M. Suzuki, The $X(3872)$ boson: Molecule or charmonium, *Phys. Rev. D* **72**, 114013 (2005).
- [20] Y. R. Liu, X. Liu, W. Z. Deng, and S. L. Zhu, Is $X(3872)$ really a molecular state? *Eur. Phys. J. C* **56**, 63 (2008).
- [21] C. E. Thomas and F. E. Close, Is $X(3872)$ a molecule?, *Phys. Rev. D* **78**, 034007 (2008).
- [22] X. Liu, Z. G. Luo, Y. R. Liu, and S. L. Zhu, $X(3872)$ and other possible heavy molecular states, *Eur. Phys. J. C* **61**, 411 (2009).
- [23] I. W. Lee, A. Faessler, T. Gutsche, and V. E. Lyubovitskij, $X(3872)$ as a molecular DD^* state in a potential model, *Phys. Rev. D* **80**, 094005 (2009).
- [24] L. Zhao, L. Ma, and S. L. Zhu, Spin-orbit force, recoil corrections, and possible $B\bar{B}^*$ and $D\bar{D}^*$ molecular states, *Phys. Rev. D* **89**, 094026 (2014).
- [25] N. Li and S. L. Zhu, Isospin breaking, coupled-channel effects and diagnosis of $X(3872)$, *Phys. Rev. D* **86**, 074022 (2012).
- [26] S. K. Choi *et al.* (Belle Collaboration), Observation of a Resonance-Like Structure in the $\pi^\pm \psi'$ Mass Distribution in Exclusive $B \rightarrow K \pi^\pm \psi'$ Decays, *Phys. Rev. Lett.* **100**, 142001 (2008).
- [27] X. Liu, Y. R. Liu, W. Z. Deng, and S. L. Zhu, Is $Z^+(4430)$ a loosely bound molecular state? *Phys. Rev. D* **77**, 034003 (2008).
- [28] X. Liu, Y. R. Liu, W. Z. Deng, and S. L. Zhu, $Z^+(4430)$ as a $D'_1 D^*(D_1 D^*)$ molecular state, *Phys. Rev. D* **77**, 094015 (2008).
- [29] F. Close and C. Downum, On the possibility of Deeply Bound Hadronic Molecules from single Pion Exchange, *Phys. Rev. Lett.* **102**, 242003 (2009).
- [30] T. Aaltonen *et al.* (CDF Collaboration), Evidence for a Narrow Near-Threshold Structure in the $J/\psi \phi$ Mass

- Spectrum in $B^+ \rightarrow J/\psi\phi K^+$ Decays, *Phys. Rev. Lett.* **102**, 242002 (2009).
- [31] X. Liu and S. L. Zhu, $Y(4143)$ is probably a molecular partner of $Y(3930)$, *Phys. Rev. D* **80**, 017502 (2009).
- [32] S. Uehara *et al.* (Belle Collaboration), Observation of a χ'_{c2} Candidate in $\gamma\gamma \rightarrow D\bar{D}$ Production at BELLE, *Phys. Rev. Lett.* **96**, 082003 (2006).
- [33] B. Aubert *et al.* (BABAR Collaboration), Observation of a Broad Structure in the $\pi^+\pi^-J/\psi$ Mass Spectrum Around 4.26-GeV/ c^2 , *Phys. Rev. Lett.* **95**, 142001 (2005).
- [34] G. J. Ding, Are $Y(4260)$ and $Z_2^+(4250)$ D_1D or D_0D^* hadronic molecules? *Phys. Rev. D* **79**, 014001 (2009).
- [35] M. Cleven, Q. Wang, F. K. Guo, C. Hanhart, U. G. Meißner, and Q. Zhao, $Y(4260)$ as the first S -wave open charm vector molecular state? *Phys. Rev. D* **90**, 074039 (2014).
- [36] Q. Wang, M. Cleven, F. K. Guo, C. Hanhart, U. G. Meißner, X. G. Wu, and Q. Zhao, $Y(4260)$: Hadronic molecule versus hadro-charmonium interpretation, *Phys. Rev. D* **89**, 034001 (2014).
- [37] Z. F. Sun, Z. G. Luo, J. He, X. Liu, and S. L. Zhu, A note on the $B^*\bar{B}$, $B^*\bar{B}$, $D^*\bar{D}$, $D^*\bar{D}$ molecular states, *Chin. Phys. C* **36**, 194 (2012).
- [38] Z. F. Sun, X. Liu, M. Nielsen, and S. L. Zhu, Hadronic molecules with both open charm and bottom, *Phys. Rev. D* **85**, 094008 (2012).
- [39] B. Hu, X. L. Chen, Z. G. Luo, P. Z. Huang, S. L. Zhu, P. F. Yu, and X. Liu, Possible heavy molecular states composed of a pair of excited charm-strange mesons, *Chin. Phys. C* **35**, 113 (2011).
- [40] L. L. Shen, X. L. Chen, Z. G. Luo, P. Z. Huang, S. L. Zhu, P. F. Yu, and X. Liu, The molecular systems composed of the charmed mesons in the $H\bar{S} + H.c.$ doublet, *Eur. Phys. J. C* **70**, 183 (2010).
- [41] R. Chen, X. Liu, Y. R. Liu, and S. L. Zhu, Predictions of the hidden-charm molecular states with four-quark component, *Eur. Phys. J. C* **76**, 319 (2016).
- [42] R. Aaij *et al.* (LHCb Collaboration), Amplitude analysis of $B^+ \rightarrow J/\psi\phi K^+$ decays, *Phys. Rev. D* **95**, 012002 (2017).
- [43] X. Liu, Z. G. Luo, and S. L. Zhu, Novel charmonium-like structures in the $J/\psi\phi$ and $J/\psi\omega$ invariant mass spectra, *Phys. Lett. B* **699**, 341 (2011); Erratum, *Phys. Lett. B* **707**, 577 (2012).
- [44] R. Aaij *et al.* (LHCb Collaboration), Observation of $J/\psi\phi$ Structures Consistent with Exotic States from Amplitude Analysis of $B^+ \rightarrow J/\psi\phi K^+$ Decays, *Phys. Rev. Lett.* **118**, 022003 (2017).
- [45] V. M. Abazov *et al.* (D0 Collaboration), Measurement of the Λ_b Lifetime in the Exclusive Decay $\Lambda_b \rightarrow J/\psi\Lambda$, *Phys. Rev. Lett.* **99**, 142001 (2007).
- [46] S. Jia *et al.* (Belle Collaboration), Observation of a vector charmoniumlike state in $e^+e^- \rightarrow D_s^+D_{s1}(2536)^- + c.c.$, *Phys. Rev. D* **100**, 111103 (2019).
- [47] G. Pakhlova *et al.* (Belle Collaboration), Observation of a Near-Threshold Enhancement in the $e^+e^- \rightarrow \Lambda_c^+\Lambda_c^-$ Cross Section Using Initial-State Radiation, *Phys. Rev. Lett.* **101**, 172001 (2008).
- [48] M. Ablikim *et al.* (BESIII Collaboration), Future physics programme of BESIII, *Chin. Phys. C* **44**, 040001 (2020).
- [49] J. Z. Wang, D. Y. Chen, X. Liu, and T. Matsuki, Constructing J/ψ family with updated data of charmoniumlike Y states, *Phys. Rev. D* **99**, 114003 (2019).
- [50] J. Z. Wang, R. Q. Qian, X. Liu, and T. Matsuki, Are the Y states around 4.6 GeV from e^+e^- annihilation higher charmonia? *Phys. Rev. D* **101**, 034001 (2020).
- [51] N. A. Tornqvist, From the deuteron to deusons, an analysis of deuteron-like meson-meson bound states, *Z. Phys. C* **61**, 525 (1994).
- [52] N. A. Tornqvist, On deusons or deuteron-like meson-meson bound states, *Nuovo Cim. Soc. Ital. Fis.* **107A**, 2471 (1994).
- [53] M. B. Wise, Chiral perturbation theory for hadrons containing a heavy quark, *Phys. Rev. D* **45**, R2188 (1992).
- [54] R. Casalbuoni, A. Deandrea, N. Di Bartolomeo, R. Gatto, F. Feruglio, and G. Nardulli, Light vector resonances in the effective chiral Lagrangian for heavy mesons, *Phys. Lett. B* **292**, 371 (1992).
- [55] R. Casalbuoni, A. Deandrea, N. Di Bartolomeo, R. Gatto, F. Feruglio, and G. Nardulli, Phenomenology of heavy meson chiral Lagrangians, *Phys. Rep.* **281**, 145 (1997).
- [56] T. M. Yan, H. Y. Cheng, C. Y. Cheung, G. L. Lin, Y. C. Lin, and H. L. Yu, Heavy quark symmetry and chiral dynamics, *Phys. Rev. D* **46**, 1148 (1992); Erratum, *Phys. Rev. D* **55**, 5851 (1997).
- [57] H. Y. Cheng and K. C. Yang, Charmless hadronic B decays into a tensor meson, *Phys. Rev. D* **83**, 034001 (2011).
- [58] F. L. Wang, R. Chen, Z. W. Liu, and X. Liu, Probing new types of P_c states inspired by the interaction between S -wave charmed baryon and anti-charmed meson in a \bar{T} doublet, *Phys. Rev. C* **101**, 025201 (2020).
- [59] G. Breit, The effect of retardation on the interaction of two electrons, *Phys. Rev.* **34**, 553 (1929).
- [60] G. Breit, The fine structure of HE as a test of the spin interactions of two electrons, *Phys. Rev.* **36**, 383 (1930).
- [61] E. Klempt, F. Bradamante, A. Martin, and J. M. Richard, Antinucleon nucleon interaction at low energy: Scattering and protonium, *Phys. Rep.* **368**, 119 (2002).
- [62] A. F. Falk and M. E. Luke, Strong decays of excited heavy mesons in chiral perturbation theory, *Phys. Lett. B* **292**, 119 (1992).
- [63] C. Isola, M. Ladisa, G. Nardulli, and P. Santorelli, Charming penguins in $B \rightarrow K^*\pi$, $K(\rho, \omega, \phi)$ decays, *Phys. Rev. D* **68**, 114001 (2003).
- [64] M. Cleven and Q. Zhao, Cross section line shape of $e^+e^- \rightarrow \chi_{c0}\omega$ around the $Y(4260)$ mass region, *Phys. Lett. B* **768**, 52 (2017).
- [65] X. K. Dong, Y. H. Lin, and B. S. Zou, Prediction of an exotic state around 4240 MeV with $J^{PC} = 1^{-+}$ as C-parity partner of $Y(4260)$ in molecular picture, *Phys. Rev. D* **101**, 076003 (2020).
- [66] J. He, Y. Liu, J. T. Zhu, and D. Y. Chen, $Y(4626)$ as a molecular state from interaction $D_s^*\bar{D}_{s1}(2536)-D_s\bar{D}_{s1}(2536)$, *Eur. Phys. J. C* **80**, 246 (2020).
- [67] F. L. Wang, R. Chen, Z. W. Liu, and X. Liu, Possible triple-charm molecular pentaquarks from $\Xi_{cc}D_1/\Xi_{cc}D_2^*$ interactions, *Phys. Rev. D* **99**, 054021 (2019).

- [68] Z. Y. Wang, J. J. Qi, J. Xu, and X. H. Guo, Studying the D_1D molecule in the Bethe-Salpeter equation approach, *Phys. Rev. D* **102**, 036008 (2020).
- [69] D. O. Riska and G. E. Brown, Nucleon resonance transition couplings to vector mesons, *Nucl. Phys.* **A679**, 577 (2001).
- [70] M. Tanabashi *et al.* (Particle Data Group), Review of particle physics, *Phys. Rev. D* **98**, 030001 (2018).
- [71] R. Chen, A. Hosaka, and X. Liu, Searching for possible Ω_c -like molecular states from meson-baryon interaction, *Phys. Rev. D* **97**, 036016 (2018).